B

GEOLOGICAL SURVEY OF CANADA

DEPARTMENT OF ENERGY,
MINES AND RESOURCES

PAPER 68-1
Part B

REPORT OF ACTIVITIES,

Part B: November 1967 to March 1968

Price, $1.50

1968

Technical editing and compilation
R. G. Blackadar
Layout
Dervorguilla Snowden

GEOLOGICAL SURVEY

OF CANADA

PAPER 68-1
Part B

REPORT OF ACTIVITIES,

Part B: November 1967 to March 1968

DEPARTMENT OF ENERGY, MINES AND RESOURCES

Available by mail from the Queen's Printer, Ottawa,

from Geological Survey of Canada,
601 Booth St., Ottawa,

and at the following Canadian Government bookshops:

HALIFAX
1735 Barrington Street

MONTREAL
Æterna-Vie Building, 1182 St. Catherine St. West

OTTAWA
Daly Building, Corner Mackenzie and Rideau

TORONTO
221 Yonge Street

WINNIPEG
Mall Center Bldg., 499 Portage Avenue

VANCOUVER
657 Granville Street

or through your bookseller

Price $1.50 Catalogue No. M44-68-1B

Price subject to change without notice

ROGER DUHAMEL, F.R.S.C.
Queen's Printer and Controller of Stationery
Ottawa, Canada
1968

CONTENTS

CONTENTS (cont'd)

CONTENTS (cont'd)

CONTENTS (cont'd)

ABSTRACT

This report comprises forty-four brief papers that describe research carried out by members of the Geological Survey of Canada between November 1967 and March 1968.

REPORT OF ACTIVITIES, NOVEMBER 1967 TO MARCH 1968

INTRODUCTION

The forty-four papers that comprise this report describe the results of scientific studies conducted by members of the Geological Survey between November 1967 and March 1968. Some of these reports are interim and will be superseded by more extensive presentations either in one of the Survey's publications or in one of the scientific journals. The figures that illustrate the papers that make up this report are reproduced without change from material supplied by the authors.

The report of activities is at present a semiannual publication. The section covering the period November to March includes reports on both field and laboratory investigations whereas the section covering the period April to October consists primarily of reports of field work. Together with the volume of abstracts and the index of publications these reports provide an annual résumé of the major scientific activities of the Geological Survey.

Manuscripts received: 1 May 1968

ANALYTICAL CHEMISTRY

1. ATOMIC ABSORPTION SPECTROSCOPY

Sydney Abbey

The general analytical scheme for determining total Fe, Mg, Ca, Na and K in silicates by atomic absorption spectroscopy has been worked out in detail and applied to a number of different types of sample, including the six new U. S. Geological Survey reference samples. Advantages of the method are its relative speed and simplicity, and the fact that for many silicates only 5 or 10 mg of sample is required. Limitations include diminished precision and accuracy for 'total' Fe_2O_3 values over 20 per cent, for MgO values over 30 per cent and for CaO values over 20 per cent. A second Geological Survey of Canada report describing these applications, Paper 68-20, was published in April 1968.

Versatility of the instrument has been enhanced by the replacement of the gas control unit by a more stable system, by the addition of a linear-absorbance recorder, by the use of the nitrous oxide burner, and by the installation of a variable-flow atomizer. Some of these new components have been applied in preliminary experiments on aluminum determination, and will likely prove useful for barium, strontium and other metals.

2. CARBOXYARSENAZO AND DIBROMOSULPHONAZO-III AS SELECTIVE AND SENSITIVE REAGENTS FOR THE SPECTROPHOTOMETRIC DETERMINATION OF PALLADIUM

J. G. Sen Gupta

As in the case of Arsenazo-III [1], carboxyarsenazo [2-(o-arsono-phenylazo)-7-(o-carboxy-phenylazo) chromotropic acid] and Dibromosulphonazo-III [2, 7-bis)m-bromo-o-azo-phenylsulphonic) chromotropic acid] have been found to be selective and sensitive reagents for the spectrophotometric determination of palladium.

Carboxyarsenazo (CAA) forms a strong complex with palladium (II) (the Lambert-Beer law is obeyed from 0-2.5 ppm of palladium at pH 3.4) and the colour reaction is 1.15 times as sensitive as Arsenazo-III (Ars-III). The

colour reaction of Dibromosulphonazo-III (DBS-III) with up to 1 ppm of palladium is more sensitive than those of Ars-III and CAA, but at higher concentrations of palladium the absorbance increases more slowly, coinciding with Ars-III at 1.6 ppm and then becoming less than it at still higher concentrations of palladium.

With both CAA and DBS-III palladium forms two complexes of the types MR and MR_2 (M = Metal, R = Reagent). In sodium acetate-acetic acid buffer of pH 3.4 the MR complexes of palladium with CAA and DBS-III are blue and bluish pink respectively and each has an absorption maximum at 630 mμ. The MR_2 complexes of palladium with CAA and DBS-III, in the buffer medium of pH 3.4, are purple and pink respectively, each having an absorption maximum at 625 mμ. Evaluation of dissociation constants indicates that in both cases the MR_2 complex is more stable than the MR. The MR_2 complexes are also very useful analytically. From solutions of ores or meteorites the common base metals must be separated from the associated platinum group metals by ion-exchange[1] before application of either of these methods for the determination of palladium. Other noble metals present at four times the concentration of palladium do not interfere in the determinations.

---

[1] Sen Gupta, J. G.: Arsenazo III as a sensitive and selective reagent for the spectrophotometric determination of palladium in iron and stony meteorites; Anal. Chem., vol. 39, pp. 18-22 (1967).

---

3. DETERMINATION OF FLUORINE IN SILICATE AND PHOSPHATE ROCKS, MICAS AND STONY METEORITES

J. G. Sen Gupta

In a recent publication Huang and Johns[1] have described a method for determining fluorine in silicate rocks. The significant feature of the method is that the determination is said to be possible without the separation of fluorine from possible interferences by distillation or pyrohydrolysis. Some difficulty has been experienced in applying this method to some silicate rocks, and also to samples containing high fluorine, e.g. phosphate rocks, opal glass and micas. The difficulty has been overcome by introducing modifications which have improved the stability and extended the range of the method.

In the modified method, the sample (50-500 mg) is mixed with 3.5 g of Na_2CO_3 and 0.6 g of ZnO in a 30-ml platinum crucible and heated in a muffle furnace for 30 minutes at 950-1,000°C. The crucible is cooled to

room temperature, 10-15 ml water and 3 drops of 95 per cent ethyl alcohol added, and heated on a medium hot sand bath, stirring with a teflon rod until a thin slurry is obtained. The solution is filtered through a Whatman No. 42 filter paper into a polyethylene flask, washed with hot water and the excess alkali neutralized by adding 4.2 ml of concentrated HNO_3. The solution is diluted to 100 ml and an aliquot containing less than 70 µg F is transferred to a 50-ml volumetric flask containing a mixture of 5 ml of a zirconium oxychloride solution (prepared by dissolving 0.133 g $ZrOCl_2.8H_2O$ in 5 ml water and 495 ml concentrated HCl), 5 ml of alizarol cyanine RC (1.8 mg/ml aqueous solution) and 25 ml of water. After making up to volume, the solution is allowed to stand at room temperature (1/2 hour for 50 mg and 2 hours for 500 mg original sample weight) and the absorbance is measured spectrophotometrically in a 1-cm cell at 532 mµ against a standard solution containing 100 µg F. The unknown fluorine is determined from a standard curve obtained from solutions prepared identically as above from 0-70 µg F.

The modified method has been successfully applied to silicate and phosphate rocks, micas, opal glass and stony meteorites, containing from 60 ppm to 8 per cent fluorine.

In the determination of chlorine by the recommended method of Huang and Johns, there was considerable variability in the reagent blank corrections, resulting in corresponding variability in the chlorine found in actual samples. After many experiments it was established that the following points should be strictly adhered to in order to obtain reliable results:

(1) It is absolutely essential to clean all apparatus with nitric acid to avoid contamination. Preferably, separate glassware should be used exclusively for chlorine determination.

(2) A blank should be run, and a calibration curve prepared, with every batch of samples.

---

[1] Huang, W.H., and Johns, W.D.: Simultaneous determination of fluorine and chlorine in silicate rocks by a rapid spectrophotometric method; Anal. Chim. Acta, vol. 37, pp. 508-515 (1967).

COAL RESEARCH

4. PALEOGEOGRAPHY AND FACIES ASPECTS OF THE MINTO COAL SEAM, NEW BRUNSWICK

P. A. Hacquebard and M. S. Barss

The depositional basin of the Minto coal seam can be interpreted as an abandoned river valley, bordered by pre-Minto lavas and slates. This valley was shallow, as is indicated by the paleo-slope of the basement, and trended northeast, as is revealed by the presence of four parallel sand tongues in a lithofacies map of the roof rocks.

The regional seam development, determined from a coal isopach map, shows a surprisingly regular pattern, with an elongated optimum area in the centre (Fig. 1). Petrographic correlations on ten column samples show that as time progressed the formation of coal contracted towards the centre, where the greatest thickness of 2-2 1/2 feet accumulated. This area offers the best mining possibilities. On all but the western side, the border of the depositional basin is clearly indicated, and additional reserves can only be expected to occur to the west of the known areas. It cannot be stated if a mineable thickness is present here.

The coal lithofacies is based on associations of microlithotypes (clarite, durite, etc.) and is determined by means of a four-component 'facies' diagram. From this, the facies changes that occur across the depositional basin were plotted in eleven time-rock units in a cross-section. This section shows that in the shallower, northeast part the forest-moor facies predominates, while in the deeper southwest portion the reed-moor facies is present. An open-moor facies, extending over the entire basin, is represented four times.

The paleobotanical aspects of the lithofacies types, as interpreted from miospore assemblages, support their respective assignments to specific swamp environments. The forest-moor facies originated from a largely arborescent Lycopodophyta and the reed-moor facies from a predominantly herbaceous Arthrophyta vegetation.

Sulphur, averaging 6.5 per cent, occurs mainly in finely disseminated pyrite particles. It is highest in the marginal areas where the coal is thinner (Fig. 1). No correlation with coal facies is apparent and a post-depositional origin immediately following burial of the peat bog is advocated.

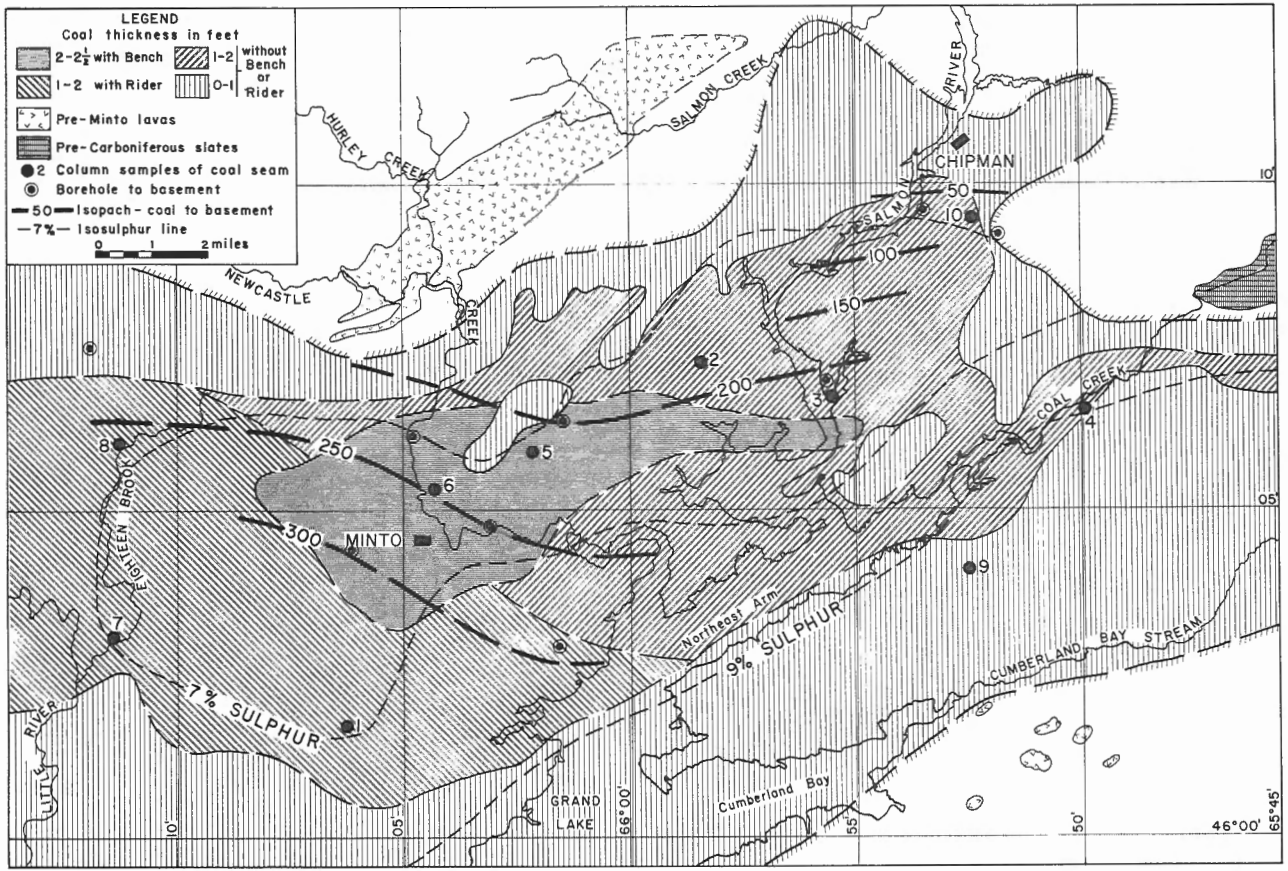

Figure 1. Paleogeographic map of the depositional sub-basin of the Minto coal seam.

The results of this investigation were presented at the 6th Carboniferous Congress held in Sheffield, England in September 1967, and will be published in the Proceedings of this Congress.

5. STRATIGRAPHY AND PALYNOLOGY OF A PERMIAN SECTION, TATONDUK RIVER, YUKON TERRITORY

E. W. Bamber and M. S. Barss

The Tatonduk River sequence is part of a 5,000-7,000-foot thick succession of upper Paleozoic rocks that forms many of the prominent topographic features in the Ogilvie Mountains near the Yukon-Alaska border, along Tatonduk River, and in the headwaters of Ettrain and Jungle Creeks.

Palynological studies, combined with macrofossil evidence, have established a Permian age for most of the stratigraphic interval involved. Accordingly, this is one of the thickest and most completely exposed Permian sections in the area. It is significant because of its proximity to the type sections of the Calico Bluff and Tahkandit Formations in Alaska, which have similar lithology.

The sequence on Tatonduk River is divisible into four units, in descending order, the Tahkandit Formation (chert, skeletal limestone, dolomite and siltstone), the middle recessive unit (siltstone, shale, limestone, and sandstone, with minor conglomerate), Rock unit B(argillaceous limestone and calcareous shale), and Rock unit A (pyritic shale and siltstone). An abundant marine fauna in the upper three units shows a Permian age (Early Leonardian – Middle Wolfcampian). Sporomorphs, which are present from near the base of rock unit A to near the top of the middle recessive unit, also indicate a Permian age. Reworked Devonian and Lower Carboniferous sporomorphs are also present.

This occurrence of Permian spores and pollen in association with a marine fauna, provides an opportunity for defining the age of the sporomorph assemblage in terms of the standard North American Marine Permian succession.

The association of reworked Devonian and Lower Carboniferous sporomorphs with those of Early Permian age, reflects erosion and redeposition during Lower Permian time which resulted in a widespread sub-Permian unconformity in the area. A possible source for the reworked sediments may have been from the north or northwest along Dave Lord Ridge and in the Nation River area of Alaska, where the most severe erosion took place, exposing the oldest rocks found beneath the sub-Permian unconformity.

ENGINEERING GEOLOGY

6. DAM SITE INVESTIGATION

E. B. Owen

A report was prepared for Inland Waters Branch, Department of Energy, Mines and Resources describing the engineering characteristics of Precambrian bedrock at four proposed dam sites in northwestern Ontario. The locations of these sites are as follows:

Albany River dam site (88° 57'W, 51° 30'N)
Attwood River dam site (88° 52'W, 51° 06'N)
Otoskwin River dam site (89° 36'W, 51° 50'N)
Pipestone River dam site (90° 35'W, 52° 17'N)

At all sites bedrock is competent and should provide satisfactory foundation and abutment material. Permeabilities computed for bedrock during the drilling of some 32 test borings at the dam sites indicate leakage could occur along joint fractures chiefly in the upper 10 feet of rock. These could be grouted.

Fragments of massive chalcopyrite up to 2 inches in diameter and associated thin seams of copper carbonate occur as float in talus on the left abutment of a proposed dam site on Yukon River immediately upstream from the Alaska-Yukon Territory boundary (141° 00'W, 64° 41'N).

EXPLORATION GEOPHYSICS

7. TIME DOMAIN AIRBORNE ELECTROMAGNETIC INTERPRETATION

A. Becker

The installation of a Time Sharing Computer Terminal has greatly simplified the task of preparing theoretical curves for the interpretation of field results obtained with the INPUT airborne system. Progress is currently being made in achieving a complete simulation of this system on the computer. Some preliminary results have already been obtained.

Figure 1 shows a theoretical transient over a homogenous half space whose conductivity is about that of sea water (1 mho/m). With the exception of the initial part, the transient is almost an exponential which decays with a time constant of about 750 microseconds.

Flying over sea water fiords Barringer[1] reports nearly exponential transients with time constants in the range of 450-720 microseconds. Unfortunately a direct comparison with the theoretical curve is not possible because the field data was obtained with a horizontal axis receiver whereas the theoretical values were computed for a vertical axis receiver.

---

[1] Barringer, A. R.: (Barringer Research Limited) INPUT system brochure; Toronto (1966).

---

8. DATA COMPILATION AND ANALYSIS (NAE PROJECT)

M. E. Bower

During 1967 analysis methods for digitally recorded aeromagnetic data were further developed. Since the beginning of the North Star project in 1963 a considerable amount of data has been acquired over the Atlantic Ocean and between Greenland and Canada, some of which has been published as total field profiles. It was not until this year, however, that the computing system was reliable enough to carry out an extensive analysis program.

Of particular interest were six flights over the Reykjanes Ridge south of Iceland. To facilitate interpretation, several different bandpass filters were used to separate anomalies of various wavelengths from the total field profiles. The profiles produced by these filters revealed much line-to-line correlation and symmetry about the ridge that could not be seen in the raw data. Another computer program was used which plots the magnetic profile of any number of dykes. By using various widths, depths and susceptibilities, one of the profiles was very closely approximated by a series of dykes. The model thus obtained was useful for studying the pattern of ocean floor spreading and the reversals of the earth's magnetic field.

Several small test areas were flown in Alberta and in the Ottawa area to see if magnetic fine structure could be recognized and correlated with known geology. Some interesting results were obtained over the Gloucester Fault south of Ottawa; the pattern of short wavelength, small amplitude anomalies changed quite noticeably around the fault zone. They could not be seen in the total field aeromagnetic map. Anomalies of this type have also been observed in Hudson Bay, and are being investigated at the present time.

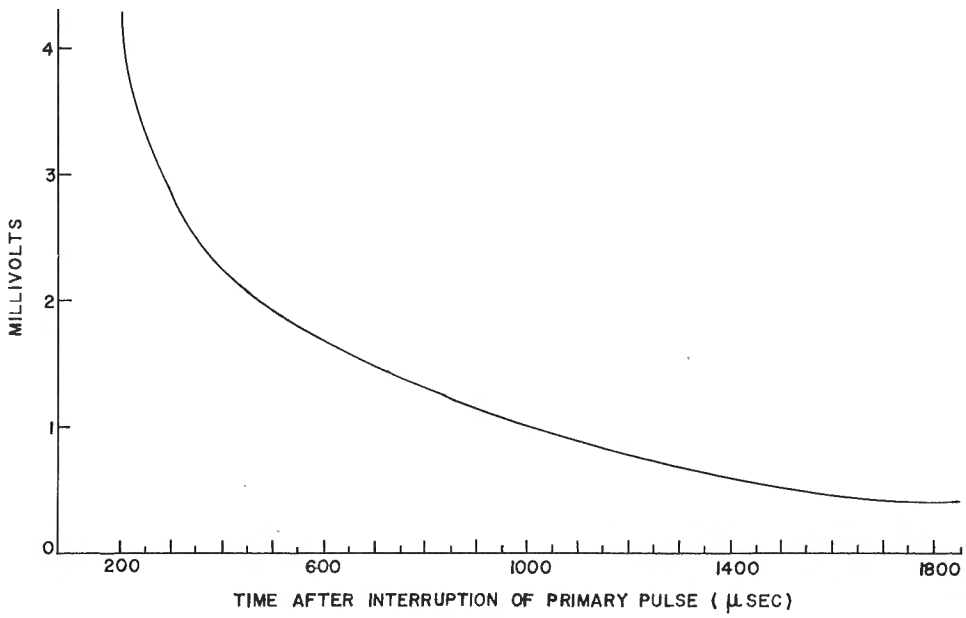

Figure 1. Approximate theoretical transient of INPUT system.

9. EVALUATION OF AIRBORNE GAMMA-RAY SPECTROMETRY IN THE BANCROFT AND ELLIOT LAKE AREAS, ONTARIO

A. G. Darnley and M. Fleet

The Geological Survey of Canada has embarked upon a project to install a highly sensitive gamma-ray spectrometer system in a STOL aircraft for the purposes of aiding geological mapping and delineating uraniferous metallogenetic provinces. This project will become operational during 1968. As a preliminary phase of this project experiments were undertaken in the summer of 1967 in the Bancroft and Elliot Lake areas of Ontario to compare ground and airborne gamma-ray spectrometry measurements. The basic premise was the necessity for thorough ground control within the area of airborne experiment. Measurements were made over two test strips 3 miles long by half a mile wide, one in each area (see Figs. 1, 2).

Ground results have been converted to corrected counts per minute for potassium-40, bismuth-214, and thallium-208. The corrections involve subtracting the background contribution, and the Compton scattering contribution in the potassium and bismuth-214 photopeaks. Radiometric contours have been plotted for each test strip, and frequency histograms have been plotted for each of the radioelements, showing the distribution patterns over the various geological formations and comparing measurements on overburden with measurements on outcrop. Intensity of radiation from outcrop and from overburden over the same rock type has been found to be closely similar. The reasons for this unexpected finding are not known at present.

Airborne measurements have been obtained with the technical assistance of Atomic Energy of Canada Limited Commercial Products, using an experimental spectrometer, with three 5 x 5-inch thallium-activated sodium iodide detector crystals, mounted in a helicopter. Atomic Energy of Canada Limited recorded the full gamma spectrum on magnetic tape, and a computer program was used in the laboratory to select, correct, and print out results. Ground and airborne results are compared in profile form, and close agreement has been demonstrated. Airborne profiles have been obtained at different elevations and attenuation coefficients determined.

There appears to be no fundamental reason why, with careful calibration, airborne data cannot be compiled so as to provide radiometric contours in terms of absolute abundance of potassium-40, bismuth-214 and thallium-208 at ground level.

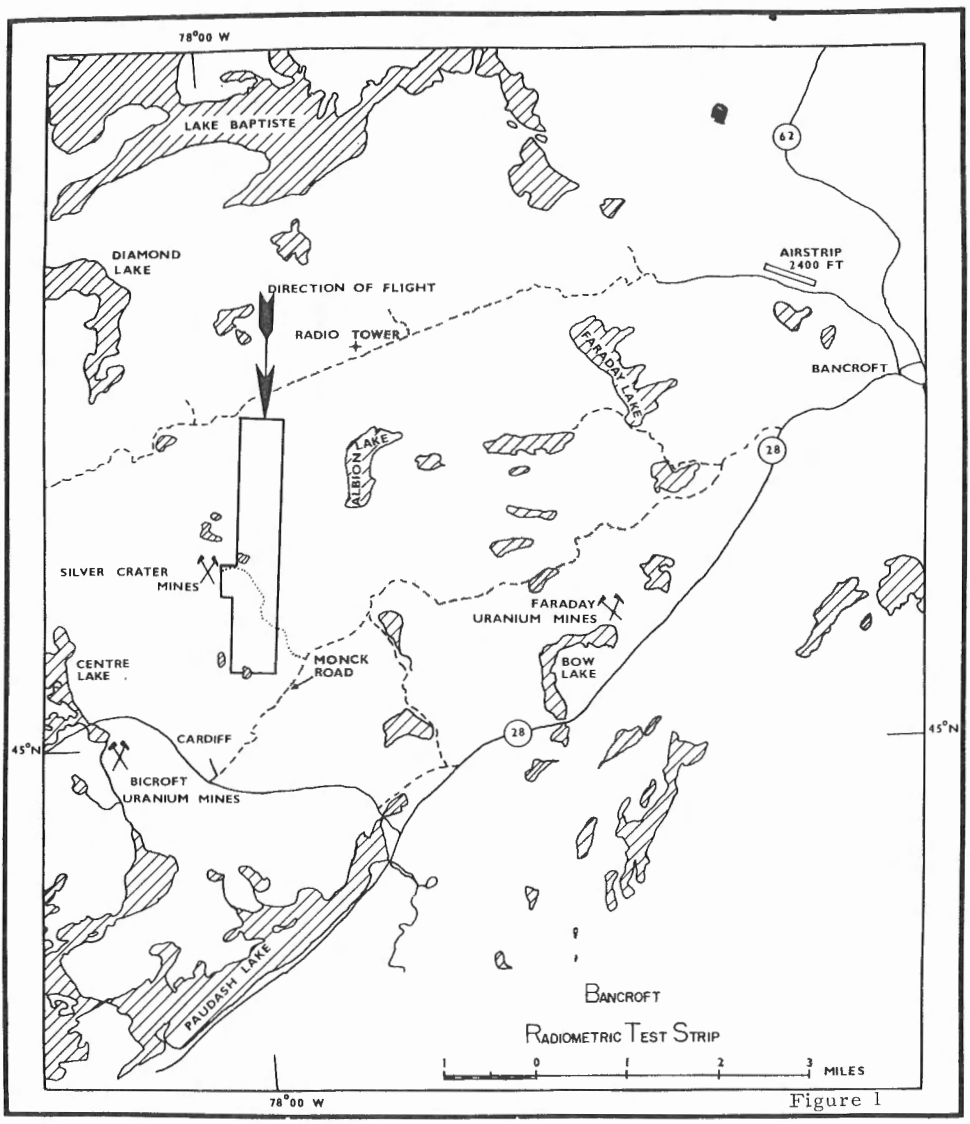

Figure 1

Arising from the observed distribution frequency histograms over different rock-types there is some evidence to suggest that characteristic radiometric signatures may be derived from airborne measurements over a variety of rock types, and that these will render identification of these rock types possible from the air. It is probable that the practical application of this technique will require simultaneous photo interpretation to provide information as to the boundaries of rock units.

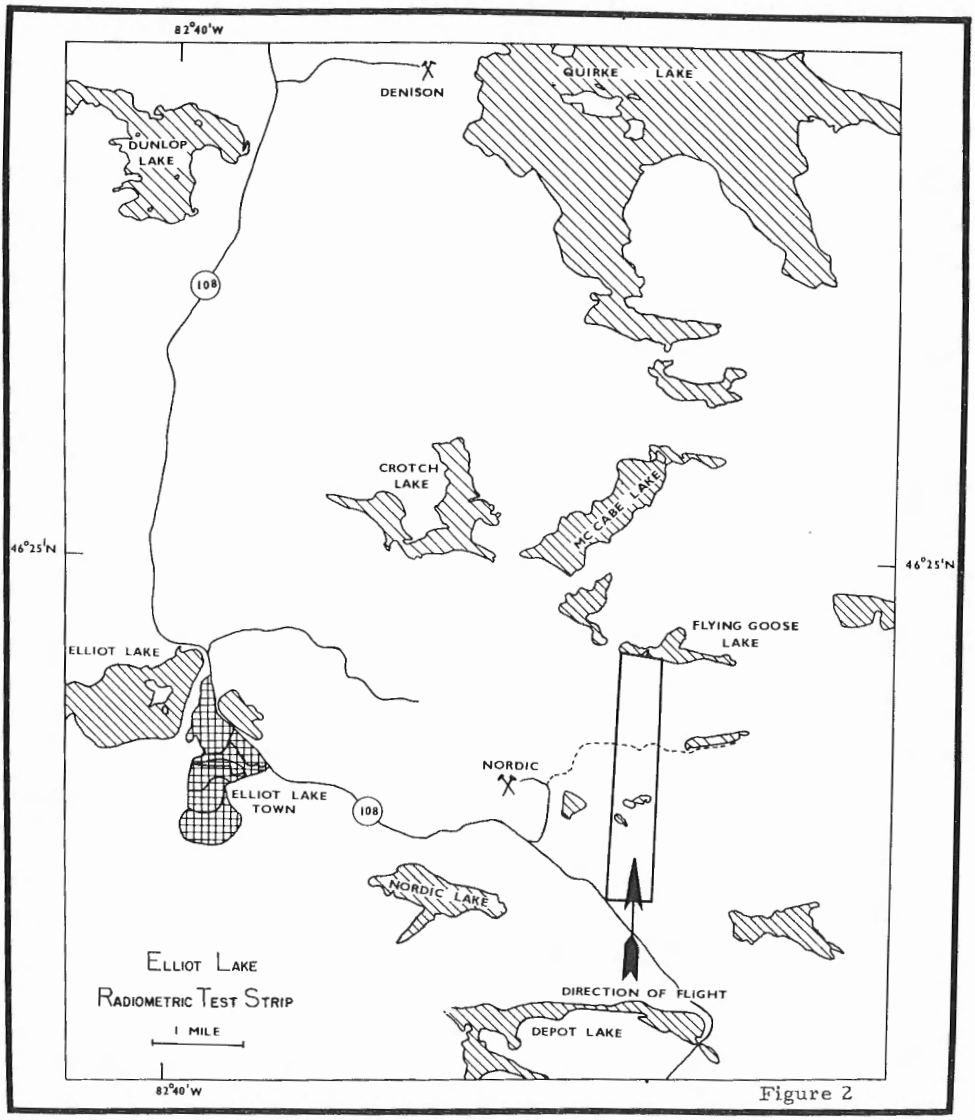
82°40'W
DENISON
QUIRKE LAKE
DUNLOP LAKE
108
CROTCH LAKE
MC CABE LAKE
46°25'N
46°25'N
FLYING GOOSE LAKE
ELLIOT LAKE
NORDIC
ELLIOT LAKE TOWN
108
NORDIC LAKE
ELLIOT LAKE
RADIOMETRIC TEST STRIP
1 MILE
DIRECTION OF FLIGHT
DEPOT LAKE
82°40'W

Figure 2

10. VERTICAL GRADIENT STUDIES: DIPPING DYKE CASE AND EULER'S DIFFERENTIAL EQUATION

Peter J. Hood and D. N. Skibo

With the successful development of high resolution magnetometers such as the cesium and rubidium varieties, direct measurement of the first vertical derivative of the total intensity of the earth's magnetic field in aeromagnetic surveys has become feasible[1]. Moreover there seem to be some distinct advantages in measuring the vertical gradient as well as the total field values. For instance, the diurnal variations of the earth's magnetic field are automatically removed from the recorded vertical gradient data.

In carrying out quantitative interpretations of vertical gradient anomalies, when the mathematical expression for the causative body is a homogenous function, Euler's differential equation may be employed[1, 2]. The homogenous function will be of the form,

$$\Delta T = \frac{K}{r^n}$$

Where ΔT = magnetic anomaly amplitude,

K = constant which is dependent on body geometry, intensity of magnetization contrast etc.,

r = distance between centre of causative body and magnetometer,

n = an exponent varying between 0 and 3 which depends on the causative body geometry.

Thus for a point dipole or sphere, n = 3, point pole or horizontal cylinder, n = 2, and for the dipping dyke, n ranges from 0 (wide dyke) to 1 (thin dyke). Now Euler's differential equation is

$$x \frac{\partial \Delta T}{\partial x} + y \frac{\partial \Delta T}{\partial y} + h \frac{\partial \Delta T}{\partial z} = -n \Delta T$$

where h is the depth to the causative body which will include the terrain clearance of the aircraft in aeromagnetic surveys.

The equation for the total intensity anomaly (ΔT) over an infinite dipping dyke is

$$\Delta T = 2Jbc \left[\sin \alpha \left(\tan^{-1} \frac{x+d}{h} - \tan^{-1} \frac{x-d}{h} \right) - \frac{\cos \alpha}{2} \log_e \frac{(x+d)^2 + h^2}{(x-d)^2 + h^2} \right]$$

..... (Hood, [3])

using an origin at the centre of the dyke, x and y axes at right angles to the strike and parallel to the dyke respectively, and z axis vertically downwards; J is the total intensity of magnetization of the dyke, and d is the half-width of the dyke whose top is at depth h below the origin; also

$$\alpha = (\lambda + \nu - \theta) \text{ where } \tan\lambda = \frac{\tan I}{\cos A},$$

$$\tan\nu = \frac{\tan i}{\cos a},$$ and θ is the dip of the dyke; I is the inclination of the earth's magnetic field, A is the horizontal angle between the x axis and magnetic north, i and a are the inclination and the horizontal declination angles of the magnetization vector J with respect to the coordinate axes;

also $b = (\sin^2 i + \cos^2 i \cos^2 a)^{1/2}$

and $c = (\sin^2 I + \cos^2 I \cos^2 A)^{1/2}$

It can be seen that the equation for the total intensity anomaly over a dipping dyke is not homogenous, so that Euler's differential equation does not strictly apply. However it is still possible to calculate a value of the exponent n which is an indication of the rate of fall-off of the anomaly with height. This procedure has been used by Slack et al.[2] to distinguish between intrabasement intrusive-type features ($n < 2$) and suprabasement-type features ($n > 2$) with which the uplift of overlying sediments may be associated and thus provide the possibility of a structural oil trap.

The general expression for the vertical gradient of the total intensity anomaly over a dipping dyke is

$$\frac{\partial \Delta T}{\partial z} = 2Jbc \sin\theta \left[\frac{(x-d)\sin\alpha + h\cos\alpha}{(x-d)^2 + h^2} - \frac{(x+d)\sin\alpha + h\cos\alpha}{(x+d)^2 + h^2} \right]$$

also the horizontal gradient of the total intensity anomaly at any point is

$$\frac{\partial \Delta T}{\partial x} = 2Jbc \sin\theta \left[\frac{(x-d)\cos\alpha - h\sin\alpha}{(x-d)^2 + h^2} - \frac{(x+d)\cos\alpha - h\sin\alpha}{(x+d)^2 + h^2} \right]$$

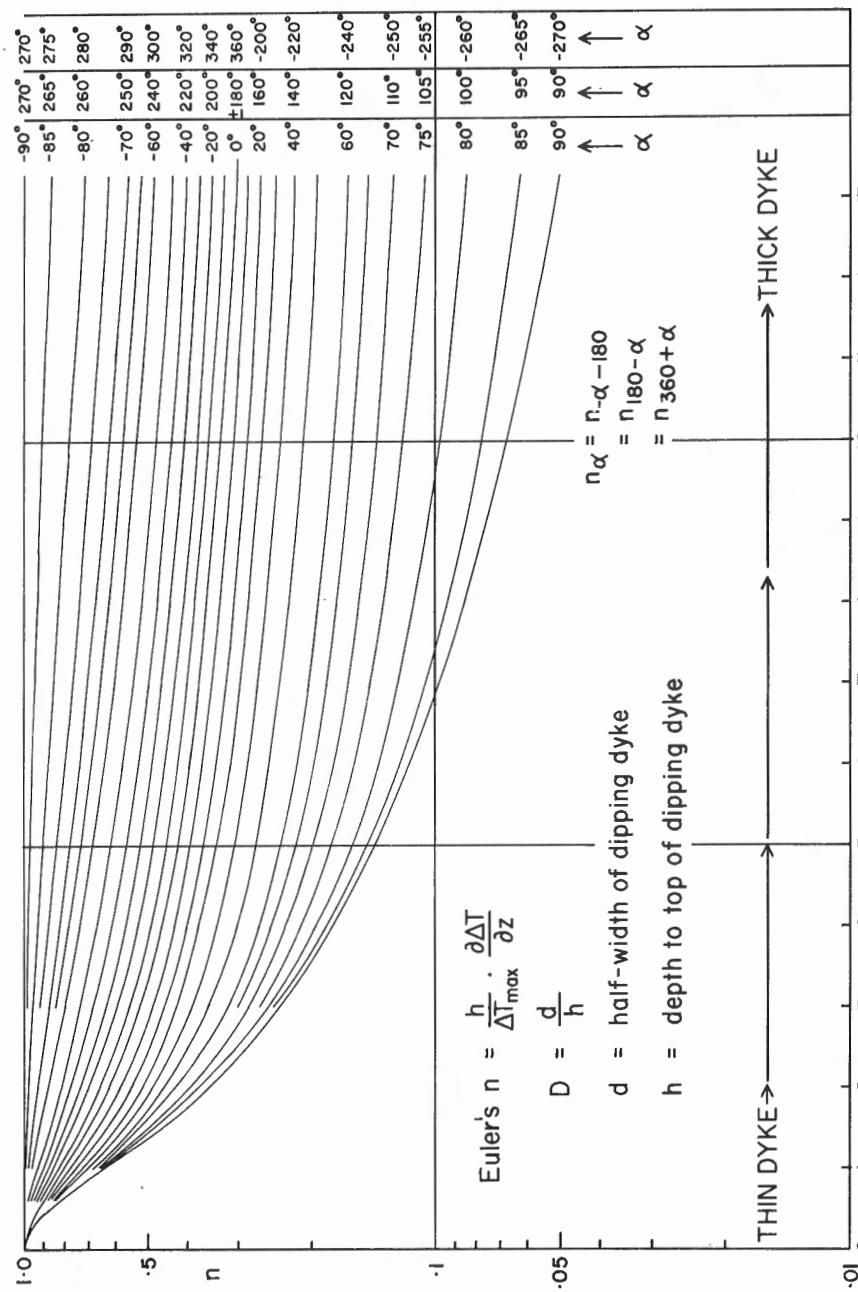

Figure 1. Graph showing family of curves for Euler's n plotted against the half-width (D) in depth units of a dipping dyke for various values of the parameter α.

Because the y axis of the coordinate system is parallel to the dyke, Euler's differential equation for the dipping dyke case reduces to

$$x \frac{\partial \Delta T}{\partial x} + h \frac{\partial \Delta T}{\partial z} = -n \Delta T$$

since $\frac{\partial \Delta T}{\partial y} = O$

Substituting from above we have

$$n = \frac{2Jbc\sin\theta}{\Delta T} \left[\frac{(x^2+h^2)\cos\alpha - d(x\cos\alpha + h\sin\alpha)}{(x-d)^2 + h^2} - \frac{(x^2+h^2)\cos\alpha + d(x\cos\alpha + h\sin\alpha)}{(x+d)^2 + h^2} \right]$$

Putting $X = \frac{x}{h}$ and $D = \frac{d}{h}$

We obtain the normalized equation

$$n = \frac{2Jbc\sin\theta}{\Delta T} \left[\frac{(X^2+1)\cos\alpha - D(X\cos\alpha + \sin\alpha)}{(X-D)^2 + 1} - \frac{(X^2+1)\cos\alpha + D(X\cos\alpha + \sin\alpha)}{(X+D)^2 + 1} \right]$$

This dimensionless equation has been used to plot families of curves for n versus X and α. Figure 1 shows the family of curves for Euler's n for various values of D and α where ΔT is a maximum i.e. $\frac{\partial \Delta T}{\partial x} = O$

so that $n = \frac{h}{\Delta T_{max}} \frac{\partial \Delta T}{\partial z}$

This graph shows that the value of Euler's n varies with the magnetic latitude and strike of the dyke i.e. all the angles I, A, i, a, and θ which contribute to α. It should be noted however that for thin dykes the value of n is quite close to being unity irregardless of α. This is because the equation for the thin dipping dyke case is homogeneous.

Actually the conclusions reached in this short dissertation do not agree with those of Slack et al.[2]. Their results (see for instance Fig. 9 in their paper) seem to indicate that for the thin dyke case the upper limit of n is 2.0, whereas our study indicates that n cannot exceed 1.0 for the dipping dyke case.

---

[1] Hood, P.J.: Gradient measurements in aeromagnetic surveying; Geophysics, vol. 30, pp. 891-902 (1965).

[2] Slack, H.A., Lynch, V.M., and Langan, L.: The geomagnetic gradiometer, Geophysics, vol. 32, pp. 877-892 (1967).

[3] Hood, P.J.: The Königsberger ratio and the dipping dyke equation; Geophys. Prosp., vol. 12, pp. 440-456 (1964).

---

11. REGIONAL MAGNETIC SUSCEPTIBILITY SURVEY IN MANITOBA AND SASKATCHEWAN

L. J. Kornik

The first completed portion of a continuing regional survey, initiated in 1966, covers northwestern Manitoba and northeastern Saskatchewan (Fig. 1). Sample sites were visited with a float-equipped Cessna 180 aircraft. At each sample site in situ magnetic susceptibility readings, an oriented drill-core and a note on the rock type present were collected[1]. The oriented drill-cores were utilized in the laboratory for further magnetic susceptibility and remanent magnetization determination.

Results of the magnetic susceptibility determinations were plotted on a map and contoured at 100, 500, 1,000, and 2,000 ($k \times 10^{-6}$ emu/cc) (Fig. 2). This map has an extensive area of higher magnetic susceptibility values in the centre of the survey area which is surrounded by lower magnetic susceptibility values. The area of higher magnetic susceptibility values occurs as a broad, irregular, east-west band. Other smaller areas of higher magnetic susceptibility occur as isolated features. The large separation

between sample sites, the inhomogeneity of the rocks sampled and the difficulty of obtaining representative samples from chance locations are factors which limit the interpretation of the results to a qualitative regional comparison to the aeromagnetic data.

Remanent magnetization determinations on some of the drillcores collected were completed by Dr. A. Larochelle. A plot of these results on a map indicated a random distribution of the directions and intensities of the remanent magnetization and no meaningful patterns could be recognized. The directions and inclination of the remanent magnetization vectors were plotted on the lower hemisphere of an equal area net (Fig. 3). In contrast this statistical plot contains a striking single concentration of points around the centre of the net with a general scatter of points around this centre. This

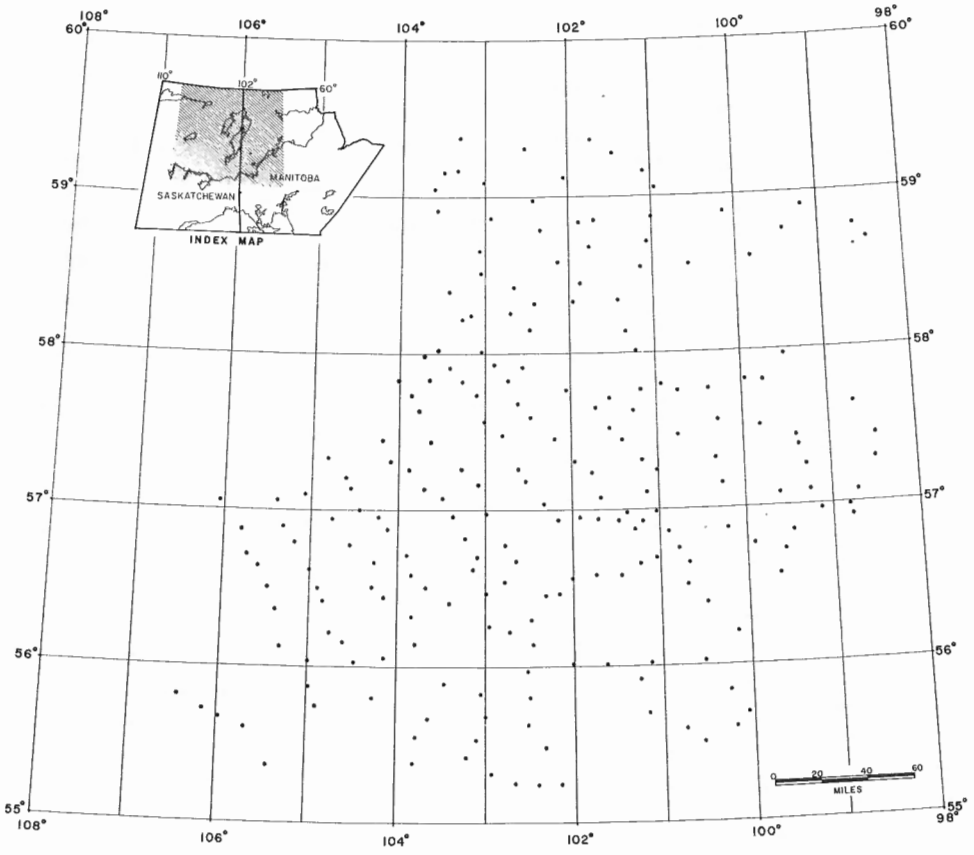

Figure 1. Map showing location of sample sites.

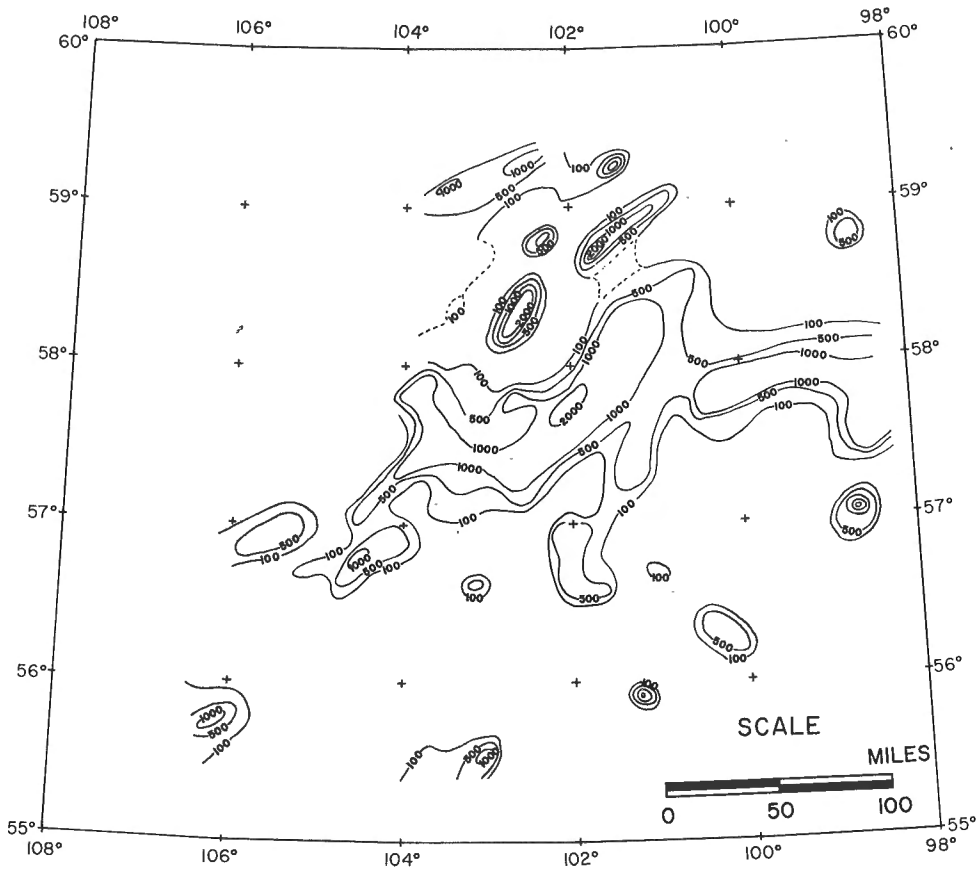

Figure 2. Magnetic susceptibility map (k x 10^{-6} emu/cc).

central concentration is high and 50 per cent of the total points lie within 20 degrees of the centre of the net. This concentration also contains the earth's present magnetic field. The statistical plot indicates a concentration of remanent magnetization vectors approximately parallel to the present earth's field and the direction of induced magnetization. The remanent magnetization would therefore simply add to the induced magnetization and would not seriously affect the induced field.

A comparison indicates that approximately 75 per cent of the drill-cores determined have intensities of remanent magnetization vectors that are lower than the magnetic susceptibilities of the same cores. Combined with the fact that the majority of the remanent magnetization vectors lie along the earth's magnetic field this suggests that the remanent magnetization of the rocks can be ignored in the regional study.

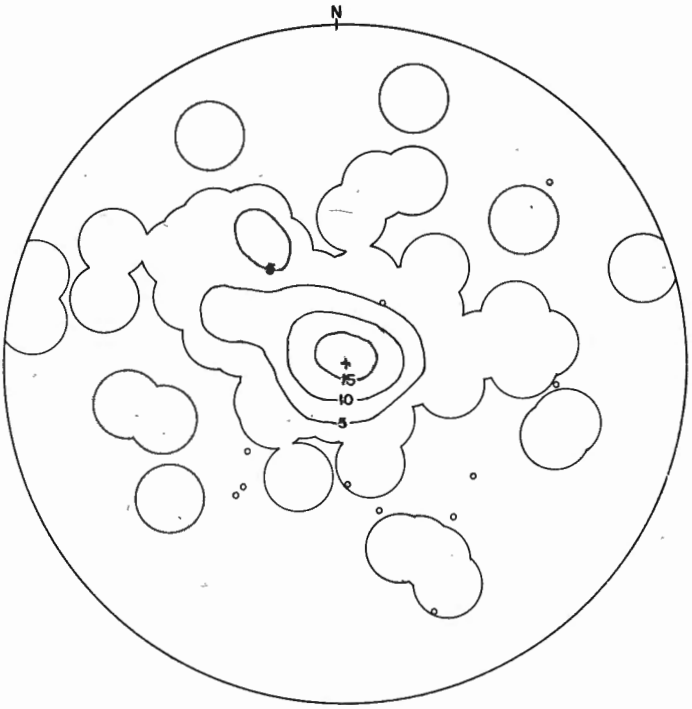

Figure 3.

Stereographic projection of remanent magnetization vectors. 104 points total contoured at 1-5-10-15 points per 1% area; 11 open circles represent ends of upward pointing vectors.

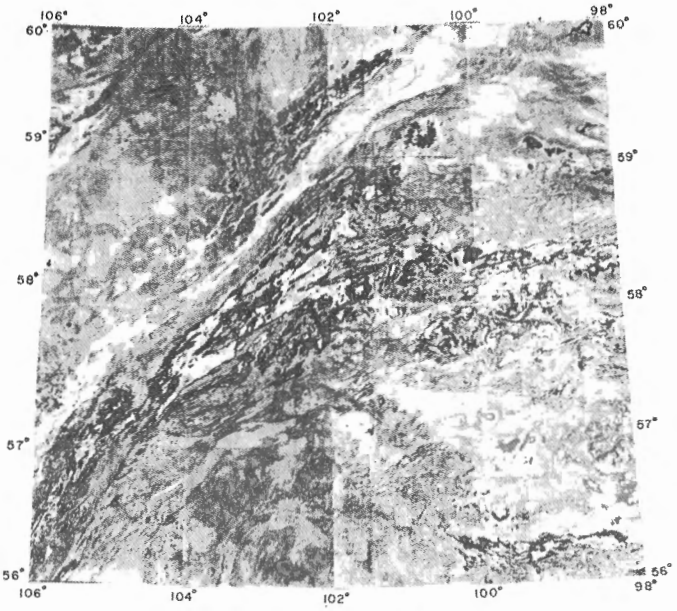

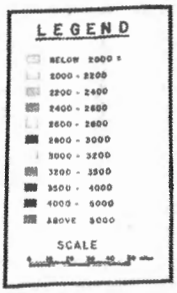

Figure 4.

Total field aeromagnetic map.

A grey tone photographic print of the coloured total field aeromagnetic map is presented for the greater portion of the survey area (Fig. 4). A comparison of Figures 2 and 4 shows a good general correlation of the main features. The large aeromagnetic high anomaly, the Owl River 'high'[2], which crosses the survey area is coincident with the large area in Figure 2 which is underlain by rocks with a higher magnetic susceptibility than rocks from surrounding areas. Rocks with higher magnetic susceptibilities are usually in an area of greater magnetic intensity. Results of the survey indicate that the aeromagnetic anomaly pattern can be correlated with the magnetic susceptibility of the underlying rocks. The ultimate aim of the survey is to establish a framework for the integration of aeromagnetic features and anomaly patterns with other types of data and to present an interpretation of regional structures.

---

[1] Kornik, L. J.: Regional magnetic susceptibility survey in Manitoba and Saskatchewan; in Report of Activities, Part A: May to October, 1966, Paper 67-1, pp. 126-128 (1967).

[2] Kornik, L. J., and MacLaren, A. S.: Aeromagnetic study of the Churchill-Superior boundary in Northern Manitoba; Can. J. Earth Sci., vol. 3, pp. 547-557 (1966).

---

12. THIN DIPPING DYKE: A RAPID GRAPHICAL METHOD OF MAGNETIC INTERPRETATION

P. H. McGrath and Peter J. Hood

The positions of maxima, minima, and points of inflection along thin dyke magnetic anomalies may be used to determine the depth to the top of the causative body. In addition, if a dyke is magnetized by induction, and demagnetization effects are unimportant, the dip of the dyke may be ascertained. The method is applicable to most diabase dykes in the Canadian Shield.

Adopting the accepted convention of y axis parallel to strike of the dyke, z axis positive downward, ΔT axis positive upward, and the positive x axis on the north side of the strike line (see Fig. 1), the equation for the magnetic anomaly over a thin dyke is given by

$$\Delta T = 2\ Jtbc \left[\frac{h \sin\alpha - x \cos\alpha}{x^2 + h^2} \right] \qquad (1)$$

J = intensity of magnetization of thin dyke, and J = kT if remanence is negligible,

k = magnetic susceptibility contrast between dyke and country rock,

T = total intensity of the earth's magnetic field,

t = thickness of the dyke (and for the thin dyke case $t < h$),

h = depth to top of dyke,

α = $(\lambda + \nu - \theta)$ where $\tan\lambda = \frac{\tan I}{\cos A}$, $\tan\nu = \frac{\tan i}{\cos a}$,

θ = angle of dip of dyke measured from positive x axis,

λ = angle of inclination of component of I in xz plane,

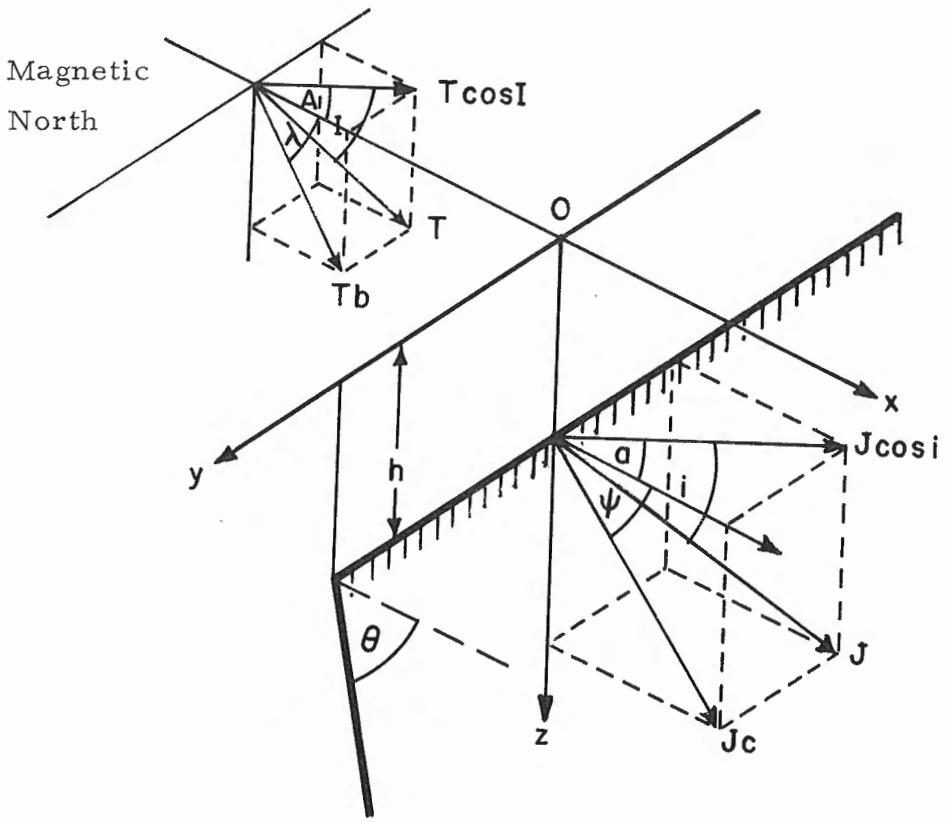

Figure 1. Oblique view of thin dipping dyke showing nomenclature used in the equation for the total intensity anomaly.

I = angle of inclination of the earth's magnetic field,

A = angle between the positive x axis and magnetic north,

i, a = the inclination and declination of J with respect to the axes,

$b = \sin I/\sin\lambda = (\sin^2 I + \cos^2 I \cos^2 A)^{1/2}$,

$c = \sin i/\sin\nu = (\sin^2 i + \cos^2 i \cos^2 a)^{1/2}$

The anomaly curve represented by equation (1) crosses over the ΔT axis at

$$\Delta T_c = \frac{2Jtbc \sin\alpha}{h} \tag{2}$$

and the x axis at

$$x_c = h \tan\alpha \tag{3}$$

Other equations which are useful in the interpretation of thin dyke anomalies are as follows (see Fig. 2).

$$x_{min},\ x_{max} = \frac{h}{\cos\alpha} (\sin\alpha \pm 1) \tag{4}$$

$$\Delta T_{max},\ \Delta T_{min} = \frac{Jtbc}{h} (\sin\alpha \pm 1) \tag{5}$$

Therefore the distance between x_{min} and x_{max} is

$$x_{min} - x_{max} = 2h \sec\alpha \tag{6}$$

and the amplitude of the anomaly is

$$\Delta T_{max} - \Delta T_{min} = \frac{2Jtbc}{h} \tag{7}$$

The solutions for the absissae of the three inflection points are

$$x_{1,2,3} = \frac{h}{\cos\alpha} \left[2\cos\left(\frac{\alpha}{3} + \beta_{1,2,3}\right) + \sin\alpha \right] \tag{8}$$

where $\beta_{1,2,3} = 210°,\ 90°,\ -30°$

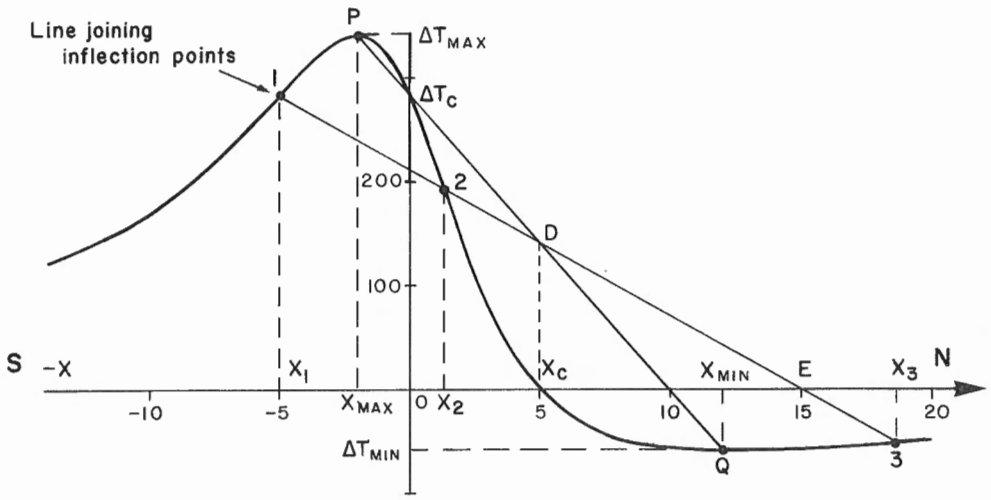

Figure 2. Total intensity profile over a thin dipping dyke showing notation used in text.

The equation of the line, PQ, joining x_{max} to x_{min} is

$$x - 2h \tan\alpha + \frac{\Delta T\, h^2}{Jtbc \cos\alpha} = 0 \qquad (9)$$

PQ intersects the x axis at 2 h tanα and the ΔT axis at the same point as the anomaly curve (equation 2).

The equation of the line joining the three inflection points is

$$x - 3 h \tan\alpha + \frac{2\Delta T\, h^2}{Jtbc \cos\alpha} = 0 \qquad (10)$$

This line intersects the x axis at 3 h tanα, and the mid-point of PQ (Point D) at

$$\Delta T = \frac{Jtbc}{h} \sin\alpha, \quad x = h\tan\alpha \qquad (11)$$

The procedure for the interpretation of a particular anomaly is as follows (see Fig. 2):

Step (1) Join the maximum and minimum points of the anomaly. As already noted PQ intersects the anomaly curve at ΔT_c, vertically above or below the origin of the coordinate system.

Step (2) Draw a vertical line through ΔT_c. This is the ordinate of the coordinate system.

Step (3) Find the mid-point D, of PQ and from this point draw a vertical line cutting the anomaly curve. It can be shown with equations 3 and 4 that this intersection point on the anomaly curve is x_c (equation 3).

Step (4) Draw a horizontal line through x intersecting the vertical line through ΔT_c to obtain the origin 0 of the coordinate system.

Step (5) On the x axis mark a point E such that $OE = 3x_c$.

Step (6) Draw a line through D and E. This line intersects the anomaly curve at its inflection points.

Step (7) Scale off the distance between the origin and x_c,

Step (8) and between x_{max} and x_{min}.

Step (9) Determine the amplitude of the anomaly $(\Delta T_{max} - \Delta T_{min})$.

A solution for the value of α is obtained by combining equations (3) and (6) giving

$$\alpha = \sin^{-1}\left[\frac{2\,x_c}{x_{min} - x_{max}}\right] \qquad (12)$$

If the remanent magnetization is negligible or is aligned with the earth's field, then $\alpha = (2\lambda - \theta)$, so that

$$\theta = 2\tan^{-1}\left[\frac{\tan I}{\cos A}\right] - \alpha \qquad (13)$$

The depth h to the top of the thin dyke may be calculated using equation (6)

$$h = \frac{1}{2}\,(x_{min} - x_{max})\,\cos\alpha \qquad (14)$$

which can be obtained if the remanent magnetization is much greater than the induced component produced by the earth's magnetic field.

For values of α approaching $\pm 90°$, the method breaks down. However, this is the case where the curve is symmetrical about the ordinate, and Peters[1] half-slope method may be used. The half-slope distance should be divided by 1.2 for the thin dyke case in order to obtain the depth to the top of the dyke.

The magnetic moment per unit area of the face of the dyke is

$$Jt = \frac{h(\Delta T_{max} - \Delta T_{min})}{2bc} \qquad (15)$$

The above method of interpretation is based on that described by Werner[2].

For cases where it is not possible to locate the minimum point Q (maximum point P) on the curve reliably, the maximum point P (minimum point Q) and its two adjacent inflection points may be used to interpret the anomaly. The positions of the inflection points should be located by a numerical method. Second differences[3] of ΔT are plotted against their positions on the x axis. The position of an inflection point occurs where the second difference curve passes through zero.

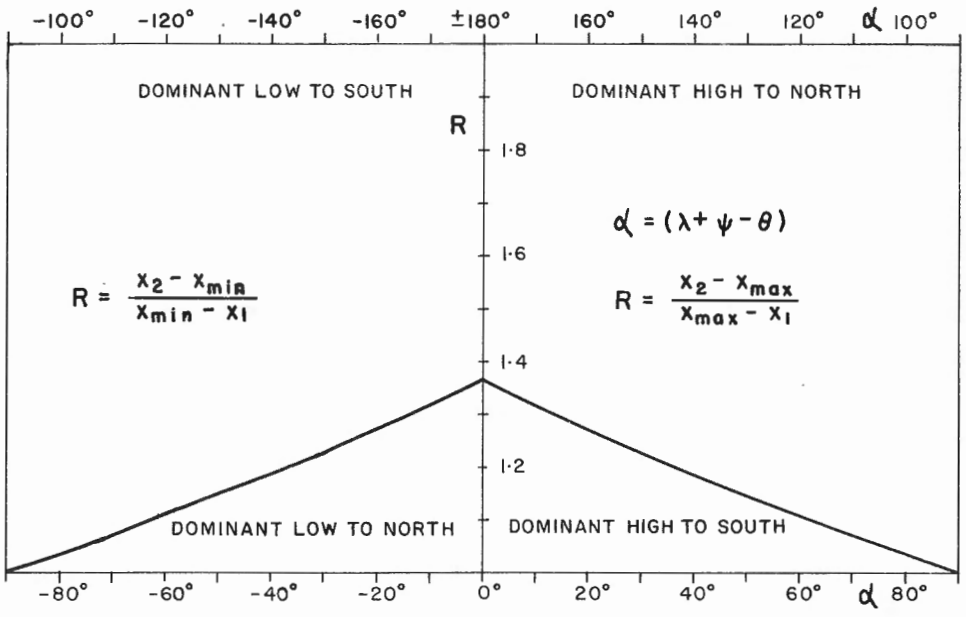

Figure 3. Curve for determination of the parameter alpha (α).

Using these three points a ratio R is defined as follows (see Fig. 2)

for dominant high $R = \frac{x_2 - x_{max}}{x_{max} - x_1}$ (16)

for dominant low $R = \frac{x_2 - x_{min}}{x_{min} - x_1}$ (17)

where x_1 and x_2 are the inflection points adjacent to x_{max} (x_{min}). The inflection point x_2 lies between x_{max} and x_{min}. If, however, it is not possible to specify the general location of x_{min} (x_{max}), x_2 is chosen such that the value of R is greater than one.

A value for the parameter α may be obtained from Figure 3 using the value obtained for R, and that range of α which corresponds to the particular case with which one is working. For instance, for the curve shown in Figure 2, which is a dominant high to the south case for the anomaly, R = 1.164. Using Figure 3 we obtain $\alpha = 45°$. From equation (13) the dip of the dyke may be determined.

In order to calculate the depth to the top of the dyke it is convenient to restrict α to the range from 0° to 90°.

It is possible to do this because of the symmetry relations which can be shown to exist[4].

$$\Delta T_{-x,\,\alpha} = \Delta T_{x,\,180-\alpha} = -\Delta T_{x,\,-\alpha} = -\Delta T_{-x,\,-180-\alpha}$$

Thus, the working value of α for calculating the depth to the top of the dyke is

Dominant high to south	$\alpha_w = \alpha$
Dominant high to north	$\alpha_w = 180 - \alpha$
Dominant low to north	$\alpha_w = -\alpha$
Dominant low to north	$\alpha_w = 180 + \alpha$

Therefore, returning to the value of $\alpha = 45°$ obtained for the curve shown in Figure 2,

$$\alpha_w = 45°$$

and from equations (4) and (8)

$$h = \frac{\cos\alpha_w (x_2 - x_m)}{1 - 2 \sin \frac{\alpha_w}{3}} \qquad (18)$$

where x_m represents x_{max} or x_{min}. Therefore using equation (18) and $\alpha_w = 45°$, a depth to the top of the disturbing body of five units is obtained.

---

[1] Peters, L.J.: The direct approach to magnetic interpretation and its practical application; Geophysics, vol. 14, pp. 290-320 (1949).

[2] Werner, S.: Interpretation of magnetic anomalies at sheet-like bodies; Stockholm, Sveriges Geologiska Undersökning, Arsbok 43 (1949); 130 p. (1953).

[3] Nielsen, K.L.: Methods in numerical analysis, p. 32; The Macmillan Company, New York, 408 p. (1964).

[4] Hood, Peter J.: The Königsberger ratio and the dipping-dyke equation; Geophysical Prospecting, vol. 12, pp. 440-456 (1964).

---

13. HIGH SENSITIVITY AEROMAGNETIC DIGITAL-RECORDING SYSTEM DEVELOPMENT

P. Sawatzky

This project is a continuation of one that began in the fall of 1964, when a group from the Geophysics Division went to work with another from the National Aeronautical Establishment (NAE) because the problems faced by the two groups were very similar. NAE's North Star, a four-engine aircraft was instrumented with a digital magnetic tape recording system that made it possible to gather all the pertinent survey data in a form that digital computers could handle. Because this aircraft is large it was possible to use off-the-shelf components. More recently this group has been working on the design and construction of a high sensitivity aeromagnetic digital system small enough to be used in a light twin-engined aircraft such as the Queenair B80.

To obtain the same capability in the B80 some very drastic instrument weight reductions had to be undertaken. Fortunately, micrologic modules became available on the market at the time that this phase of the project began. By making use of micrologic circuitry almost exclusively, the following subsystems have been designed, constructed and tested:

1. Digital clock.
2. Phase-lock tracking filter.
3. Frequency counter.
4. Shaft position decoder logic.
5. Interface between data sources and digital magnetic tape recorder.

The B80 aircraft was chosen for its overall performance. This left some unanswered questions concerning its possible undesirable magnetic characteristics. Recently, representatives from the Aeromagnetics and the Aeronautical design sections visited the Beechcraft plant in Wichita, Kansas. A rubidium magnetometer was taken along and on-the-spot checks of the magnetic properties of the B80 aircraft were undertaken at the factory. Several sources of magnetic interference were located in the aircraft. In order to transform the B80 aircraft into a suitable platform for high sensitivity aeromagnetic surveys, these sources of magnetic disturbances will have to be removed.

It is expected that the Queenair B80 aircraft will be delivered for further evaluation this summer, and after modifications have been completed it will be possible to assess this particular aircraft further as a high sensitivity survey platform.

14. INVESTIGATION OF CURIE TEMPERATURES AND SUSCEPTIBILITIES OF PRECAMBRIAN ROCKS ACROSS A RESIDUAL AEROMAGNETIC ANOMALY NEAR HALIBURTON, ONTARIO

E. J. Schwarz

After the removal of regional effects, aeromagnetic data for the Canadian Precambrian Shield show the occurrence of anomalies of wavelengths between 15 and about 100 miles and amplitudes up to about 1,000 γ [1, 2, 3]. The sources of many of these anomalies may be related to the Curie point isotherm in such a way that the magnetic crust under the magnetic 'highs' and 'lows' would be relatively thick and thin respectively. Thus, the Curie point isothermal surface may be warped due to a lateral variation in heat flow

through the earth's crust, a lateral distribution of minerals of various Curie temperatures in the crust underlying the anomalies, and possibly an increase in low-field susceptibility (Hopkinson effect) just below the Curie point at a depth of 10 to 15 miles below the residual magnetic 'highs'.

It was thought worthwhile to investigate the lateral distribution of Curie points of basement rocks across anomalies of longer wavelength in areas of predominantly vertical geological structure. Even in such areas, a downward extrapolation of the results obtained for samples collected at the earth's surface is, of course, questionable. In this note, the results are reported of Curie point determinations for Precambrian rocks collected in such an area.

The effect of the magnetic crust should also depend on lateral variations in the relative abundance of ferromagnetic minerals as well as on variations in grain size of these minerals. For that reason, the possibility of lateral variations in magnetic susceptibility measured at 20° C for surface rocks was also investigated.

A total of 58 samples was collected from the Precambrian basement around Haliburton, Ontario. The samples were taken from rocks of various types at intervals of about one mile along three sections running from a large aeromagnetic 'low' into the surrounding 'high' as shown on Figure 1. The contours of residual geomagnetic total intensity were taken from 1/63, 360 aeromagnetic maps published by the Geological Survey of Canada (numbers 146G, 99G, 104G, 110G).

The Curie temperature of small (up to about 1 g) pieces from each of the samples was determined with a simple magnetic balance of a type described earlier[4]. Some samples were also run on a recording magnetic balance of high sensitivity. The results obtained with both instruments agreed within the experimental error which generally was about $\pm$ 4° C. Some representative examples are shown on Figures 2A and 2B. The Curie point of 18 samples could not be determined accurately enough and the results for these samples were therefore discarded.

The susceptibility of most of the samples was measured in the geomagnetic field at 20° C with an induction type susceptibility meter. The limit of resolution of the instrument was 10^{-5} cgs emu.

The Curie temperatures for most of the samples range between 561 to 595° C (Table I) suggesting that the main ferromagnetic mineral is magnetite with up to a few per cent Ti. The remaining samples have Curie points between 295 and 314° C indicating the presence of ferrimagnetic pyrrhotite. The average composition of the pyrrhotite is probably slightly less Fe deficient than the ideal ferrimagnetic composition ($Fe_{0.875}S$) of which the Curie point is reported to be about 320° C (e.g. data compiled by Nagata[5]). X-ray

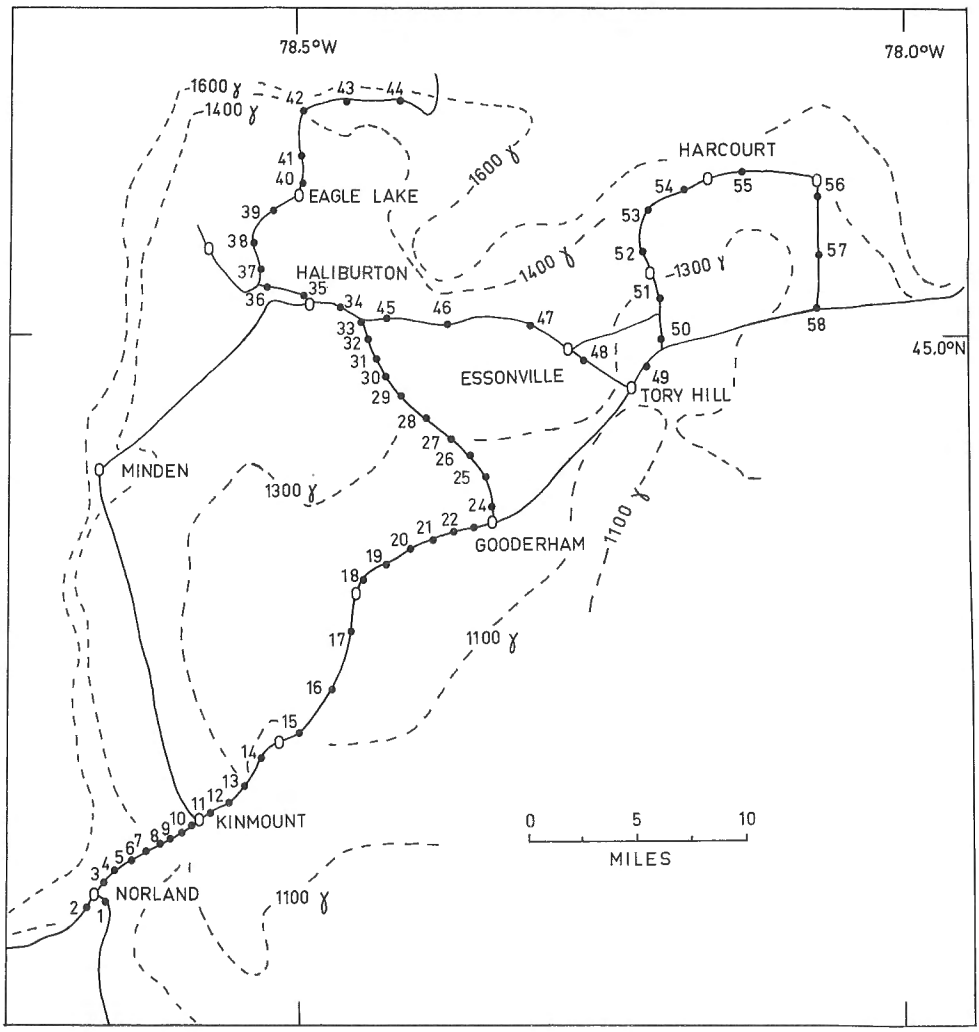

Figure 1. Map of the Haliburton area, Ontario, showing the localities of sampling and contours of regional aeromagnetic intensity.

analyses of three samples also showed the presence of magnetite and pyrrhotite. One sample contains both magnetite and pyrrhotite (Fig. 2A).

The arithmetic means of the Curie points (T_C) of the magnetite- and pyrrhotite-containing samples are given in Table II. The scatter in the distribution of the Curie temperatures is rather small.

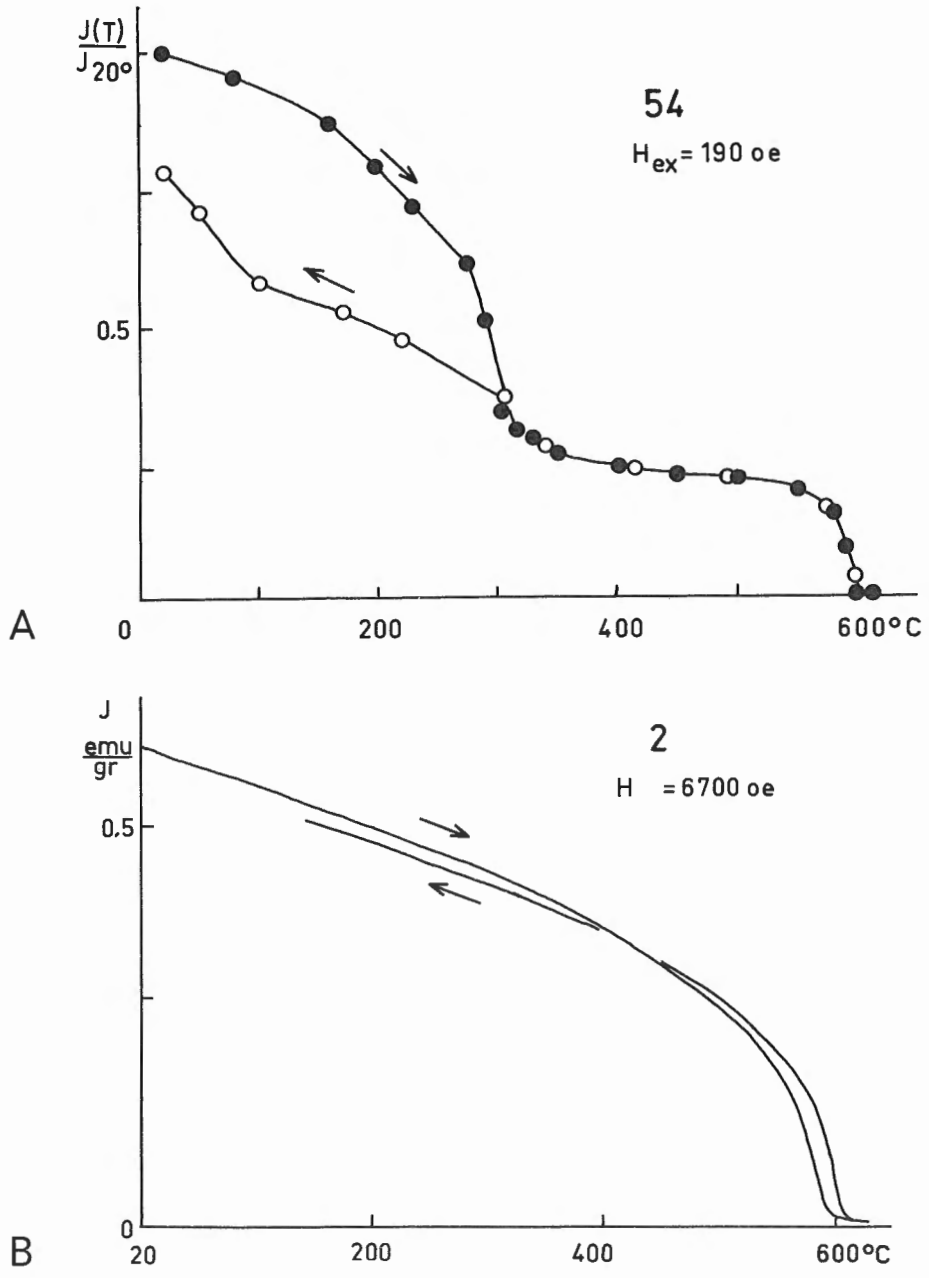

Figure 2. Thermal change of the magnetization (J) for a sample containing both pyrrhotite and magnetite (A) and a magnetite containing sample (B, continuous recording).

Table I

Experimental results for the samples. Curie temperatures are given in degrees centigrade, and the susceptibility is in cgs emu/gram.

Sample No.	Curie Temperature		Susceptibility x 10^3
2	592		1.5
5	592		3.5
6	572		0.72
7	587		1.1
9	590		2.4
10	582		1.1
11	589		1.1
12	574		5.7
13		302	0.19
17	590		2.3
18		314	2.5
19	595		3.0
20	582		0.37
25	574		4.2
26	573		0.18
27	580		4.0
28	570		0.84
29	567		2.4
30	565		7.1
31	566		0.56
32	568		1.3
33	565		1.6
34	561		0.07
35	580		
36	570		2.1
37	573		1.7
38	562		0.19
39	569		3.0
40		306	0.26
41	573		4.5
42	580		2.4
43	574		0.84
45	577		2.5
46		295	0.20
47		303	0.31
54	573	297	0.07
56	597		0.16
57	569		0.12

Table II

Statistical parameters for the three groups of data. The standard deviation is denoted by σ, the median by med., and the maximum deviation of the individual determinations from the arithmetic mean of the group by max. dev.

Group	Mean	σ	Med.	Max. Dev.	Samples
T_c magnetite	576.5°C	9.5°C	575°C	20.5°C	35
T_c pyrrhotite	303°C	6.2°C	302.5°C	11°C	6

Table III

Mean Curie point of the magnetite containing samples collected in 4 areas of different residual geomagnetic intensity (Res. Int.). Dev. G.M. indicates the deviation of each of the means from the mean of the total group (576.5°C) as given in Table II.

Res. Int.	Mean	Dev. G.M.	Samples
900-1100γ	584.3°C	7.8°C	3
1100-1300γ	576.9°C	0.4°C	10
1300-1400γ	572.2°C	4.3°C	12
1400-1600γ	580.5°C	4.0°C	10

Table III shows the mean Curie point of the magnetite bearing samples collected in each of the areas underlying the intervals of regional total intensity as shown on Figure 1. None of the means listed in Table III differs significantly from that of the mean of the whole group of magnetite-containing samples as given in Table II. The difference between each of these means and the mean of the whole group is smaller than the standard deviation of the whole group. The pyrrhotite Curie points were not included in this analysis because pyrrhotite was detected in only a few samples.

Table I shows that the scatter in the susceptibility values is very large. A large scatter is also observed if the susceptibility values are subdivided into groups according to the location of the sampling sites in each of the four areas of successively higher residual aeromagnetic anomalies as shown on Figure 1. The present data indicate that the susceptibility values do not differ significantly in these four areas.

The following conclusions may be drawn from the experimental results:

1. The main ferromagnetic minerals in the area sampled are slightly titaniferous magnetite and pyrrhotite. The small scatter in the Curie temperatures of these minerals suggests that their average chemical composition is virtually constant in the predominantly granitic-gneissic complex underlying the Haliburton region. Thus, no significant difference in the composition of the magnetite was found across the residual aeromagnetic anomalies.

2. The susceptibility data do not indicate a definite trend in the lateral variation in magnetite content across the anomalies.

3. The pyrrhotite containing samples (13, 18, 40, 46, 47, and 54) suggest the occurrence of west-northwest trending zones of sulphide mineralization in the northern part of the area sampled. The most conspicuous of these zones may be 2 miles wide (see Fig. 1).

The writer expresses thanks to Dr. L. W. Morley who suggested the study, Dr. F. Aumento who provided the X-ray results and to Mr. D. M. Rudick who assisted in obtaining the experimental results.

---

[1] Bhattacharyya, B. K., and Morley, L. W.: The delineation of deep crustal magnetic bodies from the total field aeromagnetic anomalies; J. Geomag. Geoelec., vol. 17, Nos. 3-4, pp. 237-252 (1965).

[2] MacLaren, A. S., and Charbonneau, B. W.: Characteristics of magnetic data over major subdivisions of the Canadian Precambrian Shield; Geol. Assoc. Can., vol. 19 (in press).

[3] Morley, L.W., MacLaren, A.S., and Charbonneau, B.W.: Magnetic anomaly map of Canada, 1:5,000,000 scale; Geol. Surv. Can. (in press).

[4] Schwarz, E.J.: Thermomagnetic properties of sulphide ore from the Noranda area, Canada, measured with a magnetic balance; Can. J. Phys., vol. 43, pp. 220-226 (1965).

[5] Nagata, T.: Rock magnetism, Maruzen Co., Tokyo; 350 pp. (1961).

GEOCHEMISTRY

15. A CANONICAL CORRELATION BETWEEN PHYSICAL AND CHEMICAL VARIABLES IN A CARBONATE REEF

E. M. Cameron

The relationship between a set of chemical and a set of physical variables in a carbonate reef was examined by the multivariate statistical technique of canonical correlation. Eight elements were measured on 440 samples taken from cores of the Swan Hills Member in the Swan Hills field, an important oil-producing reservoir in west-central Alberta. These variables were treated by principal components analysis, then transformed into orthogonal (varimax) factor scores which were canonically related to the physical variables: horizontal permeability, vertical permeability, porosity.

A highly significant canonical correlation of 0.58 was found between the two sets of variables. In essence, this canonical correlation comes from combining a number of weak positive and negative bivariate correlations between the orthogonal chemical factors and porosity-permeability. The three physical variables are moderately highly intercorrelated, 87 per cent of their variance being contained in their first principal component.

The canonical correlation is the product of variation in depositional environment influencing both the physical and chemical properties of the rocks and of the influence of each of these two properties on each other during diagenesis.

16. GEOCHEMICAL DISCRIMINATION BETWEEN LIMESTONE FACIES CLOSE TO AND DISTANT FROM GAS-PRODUCING DOLOMITES IN THE SLAVE POINT FORMATION

E. M. Cameron

In previous years chemical data was obtained in a regional subsurface study of the Slave Point Formation. This Middle Devonian unit, composed primarily of relatively pure calcitic limestones, produces gas in British Columbia, Alberta and the Northwest Territories mainly from porous and permeable secondary dolomites. This data is difficult to interpret by conventional methods and only with the development of suitable multivariate statistical methods has it become possible to fully understand and utilize all of the information.

Data for nine elements in sixty-nine wells penetrating the limestone facies of the formation were treated by factor analysis methods. All nine factors were extracted and factor scores were computed for each well. The wells were then separated into two groups: those lying within 2.5 miles of gas producing wells and those lying more than 2.5 miles from these wells. The scores were then used to form a discriminant equation that best separates the two groups. Four factors – Mg in calcite, Sr in calcite, clay fraction, and pyrite – account for virtually all of the discriminating power of the data. All four factors are lower in wells more distant from gas producers. The cause for these differences between the two groups is that gas is produced from dolomites and sometimes limestones of a 'reef' environment in contrast to barren 'back-reef' limestones. Greater turbulence in the 'reef' environment caused slightly less clay and pyrite to be deposited there and diagenetic leaching of the more permeable reef limestones caused a greater loss of Mg and Sr from the calcite lattice.

The wells were reclassified using the discriminant function, rather than distance from known producers. Several wells, far distant from known gas wells, were found to share very similar chemical characteristics to wells known to lie close to gas producers.

17. SEASONAL VARIATION IN RADON CONTENT OF NATURAL WATERS

Willy Dyck

To supplement radon measurements of natural waters carried out last fall in the Gatineau Hills, five creek sites and four lakes were sampled during the winter. The radon concentrations of these samples are shown in Figure 1. Although the radon content of creek waters fluctuates appreciably from one sampling time to the next, it remains relatively high throughout the winter. The radon levels in lakes in March are much higher than in September because the ice cover prevents the escape of the radon. The radon content in Pinks Lake is low compared to the other lakes. Pinks Lake is in marble, whereas the other lakes are in granitic and gneissic terrain in which uranium minerals are known to occur. Also of interest is the following order of abundance of radon under the ice at various lake sites: shore bottom > shore top > middle bottom > middle top (the Meach Lake shore samples are an exception). However, since considerable spring run-off had occurred at the time of sampling of the shore site, the result may reflect this rather than the steady state. The much higher values obtained near the shore compared to those from the middle of the lake can be explained by postulating that the radon comes from the lake sediments which have been washed into the lake by weathering and rain run-off from the surroundings, and hence reflect the

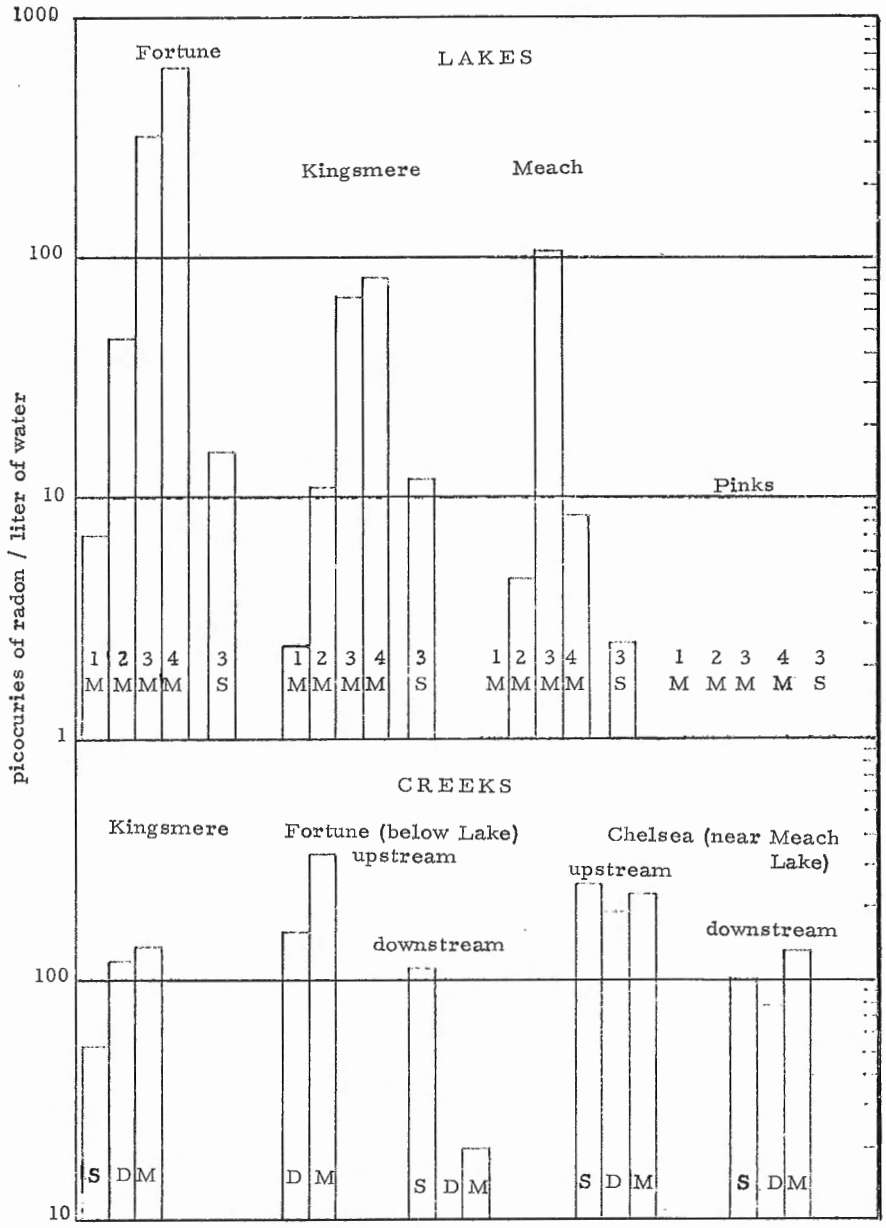

Figure 1. Radon content of lake and creek waters as a function of sampling site and time of year. Numbers 1, 2, 3, and 4 refer to middle surface, middle bottom, shore surface, and shore bottom, respectively. Letters S, D, and M refer to September, December and March, respectively.

composition of the rocks in the area. Near-shore lake sediments could thus serve, like stream sediments, as indicators of nearby mineral deposits.

18. BIOGEOCHEMICAL EXPLORATION TECHNIQUES

E. H. Hornbrook

To evaluate the effectiveness of biogeochemical exploration techniques, plant prospecting programs were carried out at one molybdenum and one copper deposit in west-central British Columbia.

The successful program at the Lucky Ship molybdenum deposit of Ammax Explorations Incorporated, where mineralization occurs in a concentric zone about a granite plug in a feldspar porphyry pluton, revealed the following major advantages of plant prospecting results for molybdenum in alpine fir needle ash. The results provide a substantially increased magnitude of anomalous to background molybdenum concentrations, an increased ground surface area of the molybdenum anomaly, and a more definite demarcation of its boundaries relative to the geochemical results of a similar B horizon prospecting program. These findings suggest that for molybdenum deposits in certain landscapes, such as the Lucky Ship deposit, biogeochemical exploration techniques can be more effective than routine geochemical B horizon exploration programs.

At the Huckleberry Mountain deposit of Kennco Explorations (Western) Limited, where copper mineralization is related to a quartz diorite stock, evaluation of the plant prospecting program results is not fully completed. However, a preliminary examination of the results shows that the distribution of copper in alpine fir needle ash indicates the extent of previously known copper mineralization.

GEOMATHEMATICS AND DATA PROCESSING

19. PREDICTION OF A COPPER-RICH ZONE IN THE WHALESBACK MINE FROM DEVELOPMENT DATA

F. P. Agterberg

The Whalesback copper ore deposit near Springdale, Newfoundland, was sampled in two stages (1) by drilling from the surface, and (2) by underground drilling.

A contour map of per cent Cu times feet for the horizontal width of the sheet-shaped orebody is shown in Figure 1. It is based on the results of 188 underground drillholes. The 100 per cent-foot contour indicates a zone which is relatively rich in copper. The zone dips about 45 degrees downward to the west. The maximum per cent-foot value in this zone is larger than 300.

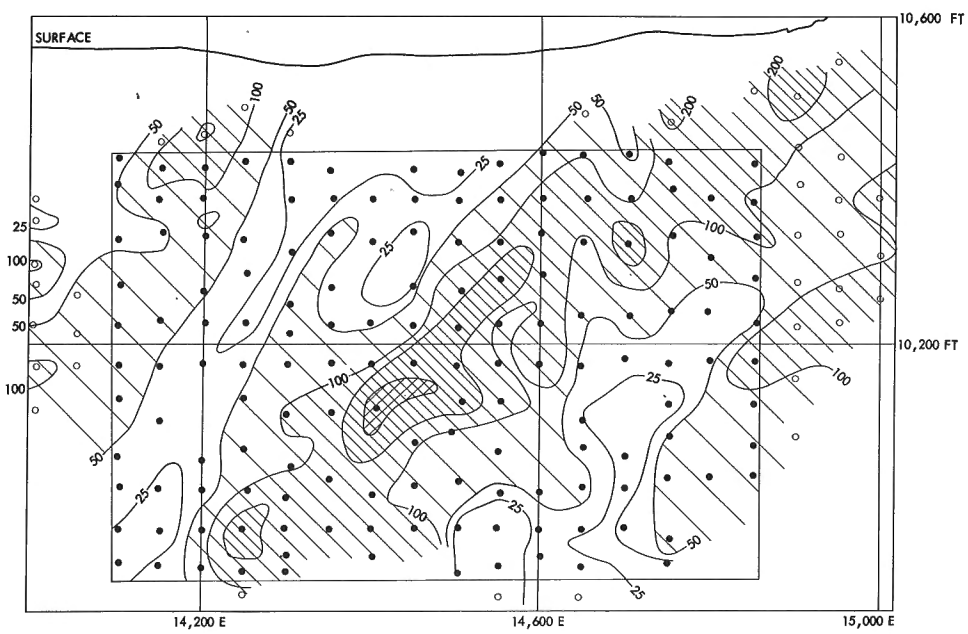

Figure 1.

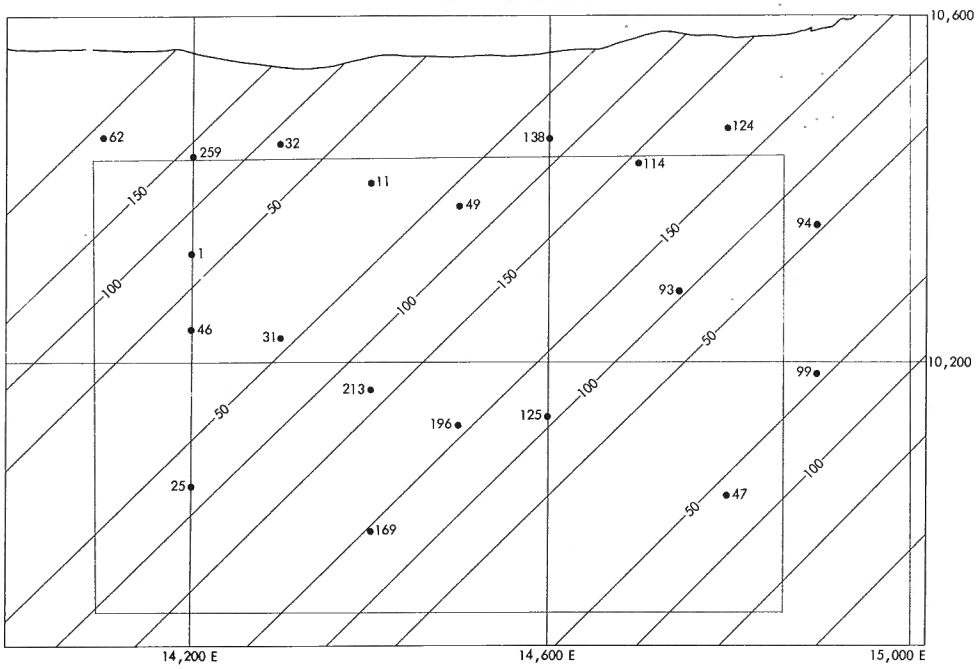

Figure 2.

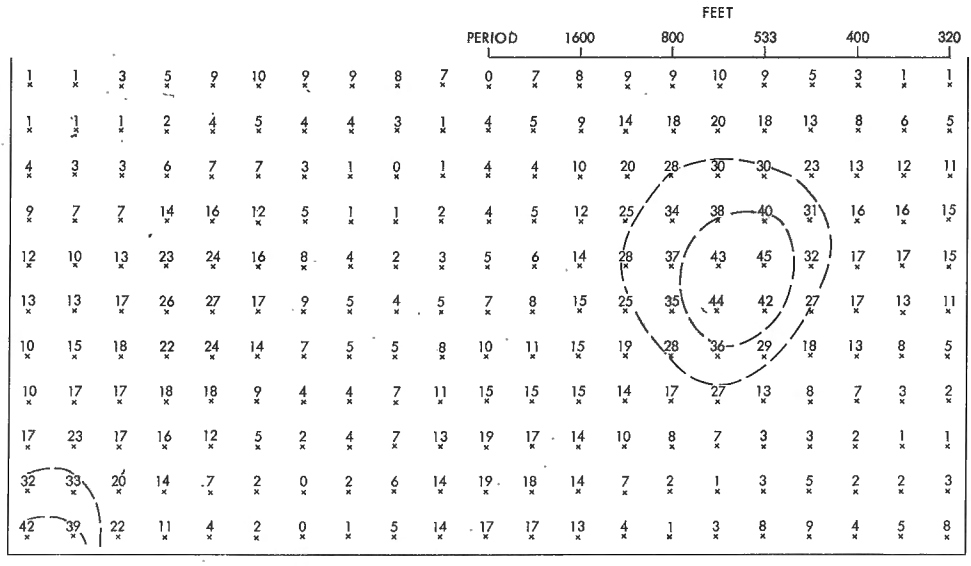

Figure 3.

The per cent-foot values for 20 holes drilled from the surface are shown in Figure 2. It can be attempted to predict the pattern in Figure 1 from this independent set of only 20 data. The following mathematical functions were fitted to the 20 data by using the method of least squares:

$$F(p, q, x, y) = A_0 + A_1 \cos G(p, q, x, y) + A_2 \sin G(p, q, x, y)$$

$$\text{where } G(p, q, x, y) = 2\pi (x/p + y/q)$$

In these equations, x and y represent the east-west direction and the vertical direction, respectively. The functions are periodic both in the x-direction (period p) and in the y-direction (period q). The values for A_0, A_1, and A_2 can be solved for given periods p and q. Each solution has a different degree of fit which can be expressed as a percentage value for the reduction in total sum of squares (Fig. 3). High values in Figure 3 mean that the degree of fit is high for the corresponding solutions. The two contours in Figure 3 that has coordinates p and q indicate solutions with a degree of fit significant at the 95 per cent and 99 per cent levels of significance, respectively.

A solution for F(p, q, x, y) with values for p and q that coincide with the most prominent peak in Figure 3 is represented in map-form in Figure 2. A comparison of Figure 2 with Figure 1 indicates that the approximate position of copper-rich and copper-poor zones can be predicted by the proposed method.

20. DEVELOPMENT OF SCIENTIFIC AND ADMINISTRATIVE ELECTRONIC DATA PROCESSING (EDP) SYSTEMS

K. R. Dawson

A. Geodat File

Development work continued on the GEODAT databank during 1967-68 and routine entry of the production of the Analytical Chemistry Section, and the Sedimentology, Isotope Geology and Carbon-14 Laboratories continued. By early December, 1967, current production had been written on magnetic tape and edited to within one step of the final form. At that time defects appeared in the complex update program and tape production was halted until Computer Sciences Division programmers effected the changes needed. Analytical data for more than 20 thousand specimens have been written on magnetic tape. In addition, programs have been written to replace the IBM 1401 card to tape with such a program on the CDC 3100; a detailed retrieval program has been developed; norm programs and a Lambert conformable plot program have been written to work on Geodat master files. At the end of the fiscal year the program development work was almost completed.

B. NACRGS Report

At the request of Dr. J. F. Henderson the 1967-1968 edition of the report on Current Research in the Geological Sciences in Canada will be produced using techniques previously developed for the Geological Survey's reports on 'Age Determinations and Geological Studies'. It is hoped to effect an economy in production and a reduced elapse time between receipt of the questionnaires and the finished publication.

The preliminary study of the previous similar report (Geol. Surv. Can., Paper 67-58) indicated that a relatively complex text would be required, with three different formats for the main text, the author list, and the introduction respectively. It is proposed to print the masters for the main text and the author list by the EDP procedure and the table of contents and introduction by typewriter. The study also showed that the line numbering scheme must identify subjects on two levels, the authors, text units, and lines within text units. This scheme has been tested and proven successful. Publication numbers have yet to be applied to text units and related to the appropriate authors. Pagination and page justification will be the final step before the masters will be printed.

C. Personnel File

At the request of the Branch Personnel Administration, development was started on a semi-automated personnel file that can readily be updated and will provide a suitably captioned book format file for day to day use by the Personnel Administration. The details of the system were discussed and a preliminary version of the file was provided. This was updated and new information regarding educational qualifications and linguistic skills was added.

Because of the limitations of unit record equipment it was decided to have the updated file captioned and printed by the computer. This requires the use of a Fortran program that is still being written. It will produce the file in book form with one page per individual on either a cyclical or a demand basis, or the card file will be sorted and listed for one of several pieces of information as required.

D. Branch Telephone List

An IBM card-based system was developed, at the request of the Branch Personnel Administration, to simplify correction and production procedures for the Branch Telephone List. The existing list was corrected and keyed into IBM cards using the format of the most recent lists. The corrected file is printed on white paper using the Departmental IBM 407 printer equipped with a new ribbon. The resulting sheets are transferred to multilith masters by the xerox machine and the desired number of copies are printed by the multilith process.

Corrections are either added to existing cards of which there is one for each name listed, or the entry is corrected by replacing the card by a new one. The file is sorted into groups by division and printed. The resulting lists are circulated to the division offices, corrected and returned to the Data Processing Unit. The file is again updated, resequenced alphabetically and printed on white paper. The printed output is forwarded to the Branch Personnel Administration where it is processed for circulation throughout the Branch.

21. NATIONAL DATA INDEX

B. A. McGee

The National Data Index is a project initiated by the Ad Hoc Committee on Storage and Retrieval of Geological Data in Canada. The Geological Survey of Canada has supplied the necessary support to initiate operation of the Index on a pilot project basis.

This office research system has two products (1) a computer-produced index to the geological data of Canada and (2) a thesaurus of the terms used in this index.

The primary intellectual responsibility of the index is the selection of words that the earth scientist would use in order to retrieve a listing of pertinent documents.

Our first index publication will be one of limited distribution in July 1968.

MINERAL DEPOSITS

22. DEVELOPMENT OF DEEP SEA INSTRUMENTATION FOR THE 1968 MID-ATLANTIC RIDGE CRUISE

F. Aumento

A new dredge type, designated the GEMEG-2, has been designed and built. The new dredge, considerably sturdier than its predecessors, will provide better sample recovery facilities and additional safety mechanisms. A more detailed, closely spaced dredging program of the Mid-Atlantic Ridge at 45°N will be attempted with the new equipment.

A fully automatic miniature deep-sea camera has been designed for mounting inside the GEMEG-2 dredges; it is now in the final stages of assembly. The camera, contained in a cylinder only 2 inches in diameter and 9 inches long, will be capable of taking over 250 photographs at predetermined time intervals. An ultra-wide angle, highly luminous lens will permit the recording of large areas in front of the dredge (see Geol. Surv. Can., Paper 68-9).

23. THE MID-ATLANTIC RIDGE NEAR 45°N. IV BALD MOUNTAIN

F. Aumento

Regionally metamorphosed and metasomatized basalts, and unmetamorphosed equivalents, were recovered from the steep slopes of Bald Mountain, a north-south elongated seamount lying 60 kilometres west of the Median Rift Valley at 45°N.

Bald Mountain is an uplifted, block-faulted seamount with a north-northwesterly plunge. A recent uplift of at least 1,000 metres, and the removal by submarine erosion of 1,000 metres of extrusives have resulted in the exposure of regionally metamorphosed and metasomatized basalts. The maximum grade of metamorphism reached was that of the greenschist facies.

Metasomatism contemporaneous with metamorphism of basalts with alkaline affinities has yielded spilites; the latter still retain relics of their premetamorphic mineralogy. More advanced metamorphism in other specimens has completely destroyed their igneous characteristics, yielding

schistose textures with porphyroblastic minerals. Other basalts have only undergone zeolitization and low temperature post-deuteric alteration with the possible replacement of some of the more lime-rich zeolites by epidote and actinolite.

The plane of the western fault scarp is thought to be a dyke or sill exposed at the time of uplift of the Bald Mountain block. This intrusive sheet consists of basalts fractionated under the late-stage volatile-rich conditions often found in sills, resulting in considerable enrichment in iron and other trace metals.

Evidence from Bald Mountain suggests that repeated fracturing must occur parallel to the original tensional faults of the Median Rift Valley at locations well removed from the axis of the Mid-Atlantic Ridge. This tectonic pattern substantiates van Andel and Bowin's hypothesis that low ocean floor spreading rates are associated with brittle fracturing of the upper crustal layers.

24. FISSION TRACK DATING OF BASALTS FROM THE MID-ATLANTIC RIDGE

F. Aumento and R. L. Fleischer*

Fission track dating of basaltic glass from the Mid-Atlantic Ridge at 45°N gives results which are consistent with the hypothesis of ocean floor spreading. Dates ranging from a minimum of 10,000 to a maximum of 300,000 years have been obtained so far. A localized rate of ocean floor spreading has been calculated to be approximately 2.5 centimetres a year. Due to the small distances involved between samples, the rate of spreading determined may not be typical for the area when integrated over significantly longer distances and time intervals. Ocean floor spreading is not expected to be continuous in the strict sense of the word, but may be the result of a number of small, rapid movements; the result of such a movement may be what is being measured here.

Correlation is also possible between the magnetic anomaly pattern over the Crest Mountains at 45°N and the geochronology of the outcropping basalts. Renewed volcanic activity well removed from the axis of the Mid-Atlantic Ridge has been shown to have taken place in recent times.

* General Electric Company.

25. METALLOGENY OF VANCOUVER ISLAND

D. J. T. Carson

The late Paleozoic rocks of Vancouver Island are similar to those of the late Paleozoic Cache Creek Group of the younger western Cordillera. The area is well suited for the application of principles relating metal deposition to tectonic history (metallogeny).

Metalliferous deposits of Vancouver Island are best classified on the basis of their metal content, mineralogy, textures, physical forms, host rocks, alterations, and where applicable, related intrusions.

Classes of syngenetic eugeosynclinal deposits on Vancouver Island are ferruginous and manganiferous cherts of the Sicker Group, and cupriferous basic volcanics and vanadiferous sediments of the Karmutsen Formation. Nickel-copper in Mesozoic (?) peridotite is also syngenetic. None of the deposits of these classes is known to be economic.

Zinc-copper-lead massive sulphide deposits include Lynx (Western Mines) and Twin "J". They occur in the Sicker Group and are in 'shear zones' which are probably tightly-folded incompetent cherty tuff horizons in which axial plane cleavage approximates schistosity. They have no obvious relationship to intrusions. The metals may be syngenetic and may have been concentrated by migration to favourable structures during subsequent periods of deformation.

Iron and copper skarn deposits are numerous. Most are erratic but some such as Brynnor and Coast Copper, have been mined.

Most skarn deposits are related to intrusions of the main orogenic stage which occurred in middle to early Late Jurassic. These intrusions are stocks and batholiths ranging in composition from gabbro to quartz monzonite. During emplacement they greatly deformed their host rocks, especially limestone, and many skarn deposits are in the deformed rocks near intrusive tongues and apophyses.

Nearly all skarn deposits are related to Late Triassic limestone (Quatsino Formation) rather than Early Permian limestone of the Sicker Group. As suggested by previous authors, this may be because the former limestone is more abundant and is underlain by the Karmutsen Formation which contributed iron (and copper) to the rising intrusions. An additional factor may have been lithostatic pressure, which in middle to early Late Jurassic time was lower at the Quatsino Formation than at the Sicker limestone. This enabled the ascending intrusions to spread laterally as tongues and apophyses in the plastic limestone, once they had breached the surface of

the competent Karmutsen volcanics. Thus the ascent of many intrusions was halted at the Quatsino Formation, allowing reaction with limestone to yield skarn deposits.

Molybdenum-copper-bearing quartz veins and stockworks are related to potassic intrusions which were emplaced during the Jurassic orogeny, and in early Tertiary. Several have been explored but none is known to be economic.

Gold-quartz, porphyry copper, arsenic-carbonate, and copper-arsenic-quartz deposits occur in linear belts of Tertiary intrusive activity which probably coincide with zones of Tertiary faulting. Porphyry copper and many gold-quartz deposits are within and adjacent to subvolcanic (?) Tertiary quartz diorite-dacite porphyry-breccia intrusive complexes. Most arsenic and copper-arsenic deposits are close to sills and laccoliths of Tertiary dacite porphyry intruding the Nanaimo Group. Past production has occurred from some gold-quartz veins, mainly those at Zeballos, and the copper-arsenic deposit of Mount Washington Copper.

Other classes of known or probable Tertiary deposits include copper related to Sooke gabbro (i.e. Sunro Mine), and mercury and alunite. None of these is presently being mined.

26. APPRAISAL OF IRON ORE RESOURCES OF CANADA, UNITED NATIONS SURVEY OF WORLD IRON ORE RESOURCES

G.A. Gross

A quantitative appraisal of iron ore resources in Canada was completed for the world survey of iron ore conducted by the United Nations. Comprehensive data on iron ore resources in Canada and a chapter describing general geological characteristics of different kinds of iron ore deposits throughout the world were contributed to this survey by the writer. Chapters written by eight other panel members who surveyed iron ore resources in different parts of the world were coordinated at a three week conference session in Geneva in October and a revised edition of the 1954 United Nations Survey of Iron Ore Resources is to be published in 1968.

The appraisal work has provided comprehensive records of geological types of deposits, tabulation of measured, indicated and inferred reserves, and estimates of potential iron ore. Data on iron ore reserves and potential ore were combined to give total quantities of iron ore resources. Information on measured reserves of ore in Canada was available from published sources for most deposits and estimates of indicated and inferred

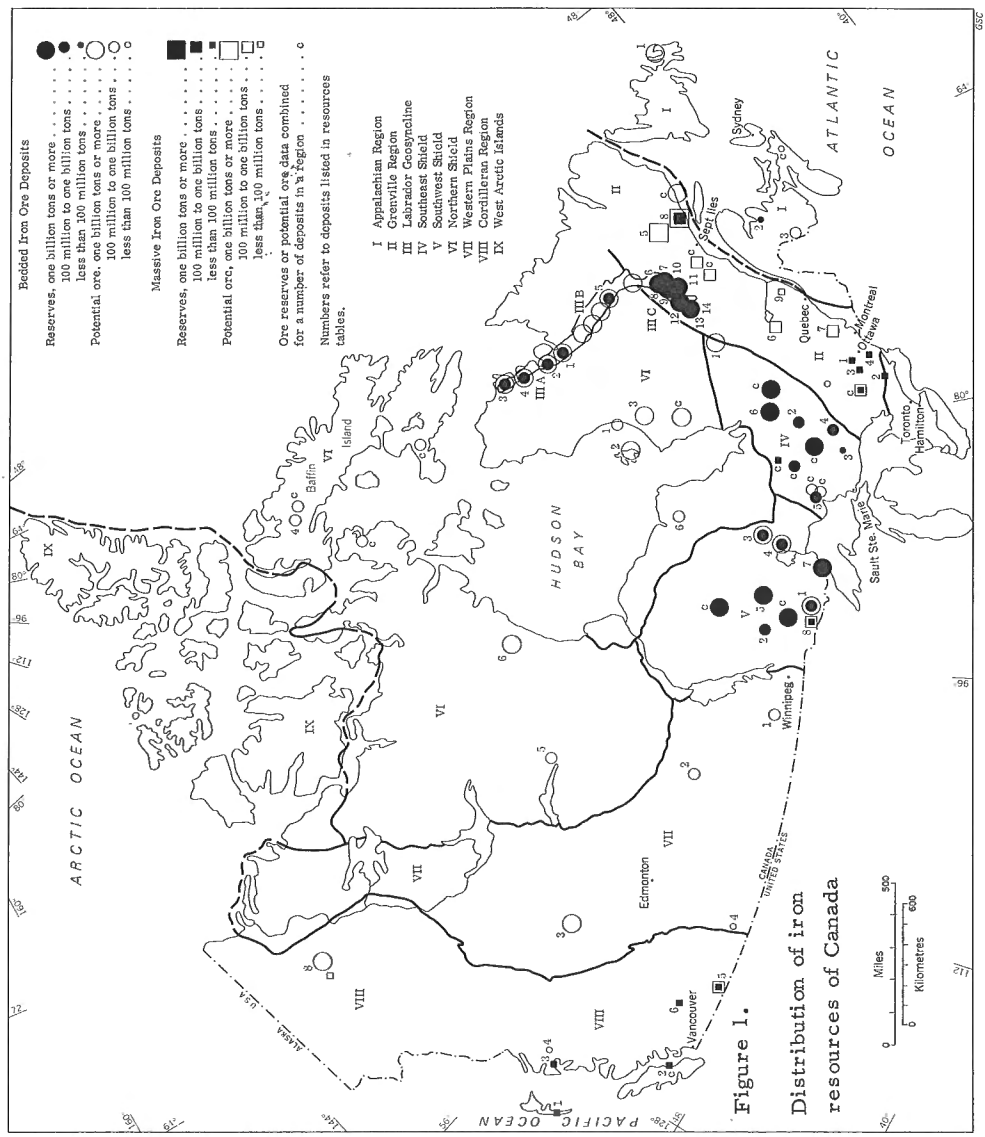

Figure 1.

Distribution of iron resources of Canada

reserves and potential ore were necessarily based to a large degree on geological knowledge of known iron deposits and their regional setting. Resources from different kinds of iron deposits in geological provinces or regions were appraised by systematic study of explored deposits and interpretation of stratigraphy, structure and other geological factors in each region.

The distribution of iron ore reserves and potential ore in Canada is shown in Figure 1 and total iron ore resources in all types of deposits in each geological region are summarized in Table 1. The total tonnage of ore reserves and estimated potential ore, the range in iron content or grade and estimates of the total iron content in deposits of various kinds are summarized in Table 2.

Table 1

IRON ORE RESOURCES IN CANADA BY REGIONS

REGION	RESERVES	IRON - Fe	POTENTIAL ORE	TOTAL RESOURCES
		in millions of metric tons		
Appalachian	10	4.5	2235	2245
Grenville	750	250	9180	9925
Labrador Geosyncline	20600	7373	32635	53235+
Southeast Shield	4805	1343	12000	16810
Southwest Shield	7295	2040	7210	14505
Northern Shield			10610	10610
Western Plains			2200	2200
Cordilleran	168	67	10325	10493
Total CANADA	33628	11077.5	86395	120023

Table 2

IRON ORE RESOURCES IN CANADA
IN VARIOUS TYPES OF DEPOSITS

(in millions of metric tons)

RESERVES			POTENTIAL ORE	TOTAL TONNAGE	
Type of Deposit and Minerals	Tons Ore	Range in Iron Content % - Fe	Tons Ore	Ore	Iron Fe
Enriched bedded hematite & goethite	1225	50.1 - 68%	1260	2485	1320
Bedded magnetite	10785	15 - 48%	33668	44453	12184.6
Bedded hematite & magnetite	20170	16 - 51.6%	40205	60375	21143
Bedded siderite-pyrite	488	20 - 38%	1950	2438	598.8
Sand magnetite	140	3.5 - 35%	2500	2640	621
Massive magnetite	369	20.2 - 59%	247	616	215
Massive Ti-magnetite & ilmenite	420	10 - 57%	6565	6985	2159
Residual hydro-hematite & others	31	47 - 50%		31	14.5
Total	33628		86395	120023	38255.9

27. METALLIC MINERAL ZONATION AROUND GRANITIC INTRUSIONS IN GASPÉ PENINSULA, QUEBEC

E. R. Rose

The writer has noted a number of interesting metallogenetic relationships with possible economic significance. One of these is the genetic relationship of important copper-molybdenum deposits to buried granitic intrusions at Copper Mountain in Gaspé Peninsula, Quebec; another is the zonal arrangement of argentiferous lead-zinc deposits about the granite core and buried intrusions of the Shickshock Mountains.

The Gaspé region is comparable to the Bingham district of Utah, which has been highly productive of lead, zinc and silver in addition to copper and molybdenum. In the Bingham district, valuable deposits of argentiferous galena and sphalerite have been found in quartz-calcite fissure veins and replacement lodes arranged zonally outwards in metamorphosed Pennsylvanian limestone beds, within a mile of the Tertiary, copper-molybdenum-bearing, Utah Copper stock[1].

Similarly, in Gaspé Peninsula, the granitic stock underlying skarn ore at Copper Mountain is host to part of the Gaspé Copper Mine which produces copper, gold, silver, bismuth and molybdenum from both porphyry copper and skarn-type deposits. To date more than 20 million tons of 2 per cent copper ore, mainly of skarn-type from nearby Needle Mountain, has been mined. Large reserves of 1 per cent copper ore of both skarn and porphyry copper types remain.

In addition, many occurrences of galena, sphalerite and minor chalcopyrite have been found in quartz-calcite veins in folded and fractured Devonian limestones, shales and other rocks, but notably west of Gaspé Mines within a 1 to 4 mile radius of the exposed granite core of the Shickshock Mountains, as shown on Map B-792, issued by the Quebec Department of Natural Resources in 1961[2]. Only one of these, the Candego Mine, on the northern flank of the Shickshock Mountains, has yet reached production, having recovered about 1.8 million pounds of lead, 1.4 million pounds of zinc, 72 thousand ounces of silver and 283 ounces of gold, from 14 thousand tons of ore milled, in the period 1948 to 1952[3]. On the southern flanks of the Shickshocks numerous galena and sphalerite-bearing quartz-carbonate veins have been explored in the Federal Mine area, clustered around a small satellitic granite stock, and small tonnages of lead-zinc-silver ore have been outlined. Other centres of mineralization may reflect underlying intrusions. Recognition of possible zonal relationships between the mineral deposits and granitic stocks may be useful in guiding exploration and prospecting in this

region and elsewhere. Geological evidence and results of exploration to date indicate important mineral potential in Gaspé Peninsula, and continuing efforts in prospecting and development are warranted.

---

[1] Hunt, R. N., and Peacock, H. G.: Lead and lead-zinc ores of the Bingham district, Utah; International Geological Congress, 18th Session, Great Britain, Pt. VII, pp. 92-96, 1948 (1950).

[2] Grenier, Paul E., et al.: Annotated bibliography of metallic mineralization in the Quebec Appalachians, and maps B-790, B-791, B-792; Quebec Dept. Nat. Resources, Mineral Deposits Branch (1963).

[3] Canadian Mines Handbooks, 1954-1967.

---

28. CANADIAN LEAD-ZINC DEPOSITS

D. F. Sangster

Progress in the study of lead-zinc deposits in Canada was mainly of two types: Documentation and Research.

Documentation

Largely through the efforts of Mrs. P. K. Shurben of the Mineral Deposits Section, the somewhat dormant lead-zinc files of the Geological Survey were re-activated, filed by NTS number, and cross-indexed by deposit name. The result was the establishment of a readily-accessible reference and data bank of more than 1,300 Canadian lead-zinc deposits or occurrences.

Research

Reportable progress in research on lead-zinc deposits centred mainly on those occurring in carbonate rocks and can be subdivided into (i) Geological and (ii) Geochemical.

(i) Geological Research

(a) Studies of the paleogeography of selected areas in Canada and elsewhere have shown that strata-bound lead-zinc deposits in carbonate rocks show a consistent pattern in their occurrence relative to sedimentary basins.

Regardless of whether the basins are marginal geosynclines or intracratonic depressions, deposits in carbonate rocks commonly seem to occur at the fringes of these basins. In marginal geosynclines such as the Appalachian or Cordilleran, mineralization occurs along the 'hinge-line' between the miogeosynclinal and eugeosynclinal areas. Where data on basement topography are available, it can be demonstrated that in carbonate rocks mineralization occurs above a change in slope of basement topography. This change of slope is frequently reflected in a change of facies in the overlying sediments (e.g. non-reef to reef; carbonate to shale) and mineralization is commonly found at or near such facies changes.

(b) In the past, production of lead and zinc in carbonate rocks has come mainly from the Proterozoic (Grenville in eastern Canada and Purcell in British Columbia) and Cambrian (Lower, Middle, and Upper in southeastern British Columbia). Recently, production has commenced in Devonian (Pine Point, Northwest Territories) and Mississippian (Walton, Nova Scotia) carbonates. Important reserves are also known to occur in the Ordovician of western Newfoundland and the Arctic Islands. Of these, lead-zinc mineralization in carbonate rocks is most widespread in the Cambrian of the Western Cordilleran Region.[1] In a 300-mile belt stretching from northern Washington State to approximately latitude 52 degrees in southeastern British Columbia (Big Bend area of the Columbia River), shelf- or miogeosynclinal-type Cambrian carbonate rocks (and their probable metamorphosed equivalents) contain at least 13 producing or past-producing mines, 5 developed or partially-developed deposits, and numerous smaller occurrences. North of the Big Bend area to the Yukon-British Columbia border, only scattered occurrences are known in Cambrian rocks. In the Ross River area of the Yukon, major lead-zinc-silver deposits are currently being developed in Cambrian eugeosynclinal[2] (?) sediments. In view of this proven potential of Cambrian sediments (both miogeosynclinal and eugeosynclinal), it would appear that Cambrian strata in the Western Cordilleran Region, north of latitude 52 degrees to the Yukon-British Columbia border, constitute one of the potentially-favourable areas for lead-zinc mineralization in Western Canada.

(c) Study of the carbonate host rocks to Canadian occurrences shows a correlation with petroleum reservoir rocks – with the exception of the Proterozoic occurrences and the strongly-folded Cambrian of southeastern British Columbia, lead-and zinc-bearing carbonate rocks also produce petroleum usually in the same sedimentary basin.

(ii) Geochemical Research

(a) In terms of bulk composition of ore, a major chemical difference exists between conformable lead-zinc deposits in carbonate rocks compared with those in volcanic rocks. Expressed as molecular ratios of Cu-Pb-Zn, deposits with carbonate as host are Cu-poor (<10 mole per cent Cu) whereas those in volcanically-derived host rocks are Pb-poor (< 20 mole per cent Pb).

(b) In studying the relationship between metal ratios in ore (Cu-Pb-Zn) and the ratios of the same elements occurring as trace amounts in the host rock carbonate, preliminary results indicate that metal ratios in the host rock remote from the deposit are similar to those in ore and that the similarity increases with increase in the size of the orebody.

(c) Quantitative analyses of sphalerite and galena concentrates (> 98 per cent pure) permit grouping of lead-zinc deposits (in carbonate rocks) according to their trace element content. In sphalerite, Cu, Ag, Mn, Cd, Ni, and Co have been used in parameters for this purpose and, in galena, Ag, Bi, and Sb seem to be the characteristic elements. Grouping of deposits by these trace elements is being studied to determine whether or not there is a correlation with geologic type, age of host rock, tectonic or metamorphic features, etc.

(d) In conjunction with the Geomathematics and Data Processing Section, computer programs have been devised to calculate and machine-plot sphalerite analyses in terms of Fe-Mn-Cd, Cu-Ag-As, and Cr-Ni-Co, galena in terms Ag-Bi-Sb, and bulk compositions of ores in terms of Cu-Pb-Zn, Pb-Zn-Ag, and Cu-Zn-Ag.

(e) Best available data on bulk composition of ore (in terms of Cu, Pb, Zn, Ag) from approximately 60 Canadian Zn- or Pb-bearing deposits have been transferred to computer data cards – each card representing one deposit. Each deposit is then machine-plotted in terms of three parameters: Cu-Pb-Zn, Pb-Zn-Ag, and Cu-Zn-Ag. These major metal ratios can then be compared for any group of deposits desired. Grouping of deposits can be by geological age of host rock, by host rock lithology, by geologic province or subprovince, by mining camps, areas, or belts, by deposit type, etc.

(f) Sulphur isotopes. Published and unpublished data continued to be reviewed and collected, as well as submitting for analysis 175 samples from selected Canadian deposits, to test the general concept that most, if not all, of the sulphur in strata-bound sulphide deposits was derived by reduction of sea-water sulphate by sulphur-reducing bacteria[3].

(g) Lead isotopes. Current and past literature on Pb-isotope studies of lead-zinc deposits was reviewed and compiled. From this emerged the general conclusion that, as a group, lead-zinc deposits in carbonate rocks, whether conformable or not, generally contain abnormal amounts of radiogenic lead compared with the calculated growth curve.

---

[1] Bostock, H. S., Mulligan, R., and Douglas, R. J. W.: The Cordilleran region, p. 284; in Geology and economic minerals of Canada; Geol. Surv. Can., Econ. Geol. Ser. 1, 4th ed. (1957).

[2] Templeman-Kluit, D. J.: Geologic setting of the Faro, Vangorda, and Swim base metal deposits, Yukon Territory; in Report of Activities, Geol. Surv. Can., Paper 68-1, Pt. A., pp. 43-52 (1968).

[3] Sangster, D. F.: Relative sulphur isotope abundances of ancient seas and strata-bound sulphide deposits; Proc. Geol. Assoc. Can., vol. 19, (in press).

MINERALOGY

29. INVESTIGATION OF RELATIVE ARGON RETENTIVITY IN SUITES OF PRIMARY POTASSIUM-BEARING MINERALS AND ASSOCIATED ALTERATION PRODUCTS

J. Y. H. Rimsaite

This is the first study performed on three paragenetically different biotites and three muscovites separated from the same rock, a nepheline syenite from Blue Mountain. For the first time successful separation was made between oxidized and unoxidized biotites and between two generations of secondary white micas that are intimately intergrown and replace nepheline. These associated micas yielded the following apparent potassium-argon ages:

1. Unoxidized and partly oxidized portions of the same biotite:
   (a) Brown unoxidized biotite K = 8.4%, 870 m.y.
   (b) Green-brown partly oxidized but otherwise unaltered biotite K = 8.26%, = 790 m.y.

2. Secondary micas replacing nepheline:
   (a) Muscovite from nepheline fractures (20-100 microns in diameter, K = 8.19%, = ca 800 m.y.)
   (b) Mica-analcite aggregate, hydronepheline (0.2-2 microns in diameter, K = 7.06%, Na_2O = 2.8%, ca 300 m.y.).

The apparent potassium-argon ages obtained on secondary micas separated from the altered nepheline provide some measure of the effect of alteration products on the age of partly altered primary minerals. Partly oxidized, brown-green biotite flakes are very common in all types of rocks and usually are not separated from brown unoxidized flakes for potassium-argon dating. This experimental work indicated that oxidation lowers the apparent potassium-argon age.

30. STUDIES OF MICAS AND HOST ROCKS

J. Y. H. Rimsaite

Geochemistry, Mineralogy and Petrology of Poly-mica Rocks

Geochemical, mineralogical and petrological studies of poly-mica rocks were initiated because of diverse isotopic age results obtained on some associated micas. Ten types of the following poly-mica assemblages were distinguished on the basis of grain size, chemical composition, mode of occurrence and alteration:

Group I. Compositional Variations within the Single Flake:

I-1 Compositional zoning.
I-2 Rims and patches of different mica.
I-3 Recrystallization and micaceous inclusions.

Group II. Different Micas in Separate Flakes:

II-1 Coarse- and fine-grained micas of similar composition.
II-2 Phlogopite-biotite.
II-3 Phlogopite (-biotite) -muscovite^{II}.
II-4 Biotite-muscovite.
II-5 Muscovite-lepidolite (biotite-lepidolite).
II-6 Primary and secondary micas.
II-7 Fresh and altered micas.

Chemical and mineralogical compositions of each type of the poly-mica rock and of the associated micas were studied with special emphasis on paragenesis and sequence of crystallization of coexisting micas. More detailed data are given in a paper prepared for presentation at the International Geological Congress and publication in IGC Proceedings, XXIII Session, Prague, Section 6 (1968.).

Study of Micas and Associated Minerals from Uncommon Rocks

Micas from two lithium-pegmatites.

Two properties of micas make them very useful minerals for the study of chemical evolution of pegmatites: (1) the ability of micas to crystallize under diverse environmental conditions and their occurrence in every zone of a zoned pegmatite, and (2) chemical complexity of micas which makes it possible to compare trends in distribution of about 20 elements in micas from various zones of a pegmatite. Furthermore, a comparison of

concentrations (atomic per cent) of the anions and cations between the mica and its host indicates origin of the mica. Distribution of the following cations and anions was studied between the mica and the host (cleavelandite, microcline, spodumene and beryl, and associated tourmaline): Si, Al, Fe^{III}, Fe^{II}, Mg, Ca, Na, K, Li, Mn, Ti, Rb, Cs, Sr, Ba, Ni, Zn, O, OH, F.

It was found that micas contain higher concentrations of the following elements than their hosts: K (except microcline), Li (except spodumene), Rb, Cs, Fe, Mn, Ni, Zn, OH, and F. Late micas are particularly enriched in Li, Rb, Cs, Mn, and F. It is concluded that the lithian micas studied did not form by simple hydration of the host and that some elements have been added. Silica is always more abundant in the host mineral, and micas that replace the host usually contain some interstitial quartz. Lithian micas, although they crystallize in relatively large flakes, are composed of very fine grained aggregates (1-50 microns) that differ in indices of refraction and in size of optic axial angles.

Natural and laboratory fused phlogopite (mica from kimberlite).

Natural occurrence of partly fused phlogopite in an eclogite nodule from a kimberlite prompted the present study of thermal stability and other chemical and physical properties of the mica and its host rock. The partly fused mica from the Kimberley mines of the Republic of South Africa is compared with Canadian micas of similar composition from basic and calcic rocks. The writer wishes to thank the De Beers Consolidated Mines Ltd. for providing the interesting specimen and for the permission to publish the analytical results of our study. The mica retains glass particles to the temperature of final dehydration, recrystallization and fusion at ca 1000°C.

Experimental Studies of Retentivity, Loss and Adsorption of Argon in partly Dehydrated Phlogopite, Biotite, Muscovite and Hydronepheline

Laboratory experiments on retentivity, loss and adsorption of argon in partly dehydrated micas (phlogopite, muscovite and hydronepheline) were continued. Results are compared with those previously obtained on biotite and the following observations made:

1. Dehydration, loss and adsorption of argon depend on chemical and physical properties of mica and on experimental conditions of dehydration.

2. Loss of radiogenic argon from the muscovite and phlogopite is proportionate to the loss of water, whereas in biotite loss of water and loss of argon are not proportionate as a result of oxidation of iron.

3. Loss of argon from the muscovite increases with increasing time of dehydration, whereas time of dehydration has less effect on loss of argon from the biotite under the experimental conditions employed.

4. Relatively coarse grained muscovite adsorbs less atmospheric argon than phlogopite and biotite of similar grain size.

5. The very fine grained micaceous alteration product, hydronepheline, adsorbs more atmospheric argon than coarse-grained muscovite, phlogopite and biotite.

Heating experiments in argon atmosphere were carried out by Mr. R. H. Lake of the Physical Chemistry Section, Mines Branch, chemical analyses by Mr. S. Abbey, Mr. J.-L. Bouvier and Dr. J. G. Sen Gupta of the Analytical Chemistry Section, Geological Survey, and isotopic studies by the staff of the Geochronology Section, Geological Survey, under the supervision of Dr. R. K. Wanless. Similar experiments on fluorine-poor phlogopite, fluorine-rich biotite, and fine-grained aggregates of lithian mica are in progress.

PETROLEUM GEOLOGY

31. AN ANALYSIS OF SIZE FREQUENCY DISTRIBUTIONS OF OIL AND GAS RESERVES OF WESTERN CANADA

R. G. McCrossan

The study which is currently underway at the Geological Survey's Institute of Sedimentary and Petroleum Geology, Calgary, was commenced with Imperial Oil Company, who gave permission to publish it and supplied much of the data used.

One of the reasons for this study was to answer the question "Are the giant pools unique geologically?" The answer seems to be that they are not, but are only rare because of the nature of the log-normal distribution. To pursue this further, it should be clear that any classification of oil pools into size ranges, even of a qualitative type, such as giant, large, medium, and small must be based on a logarithmic scale; that is a multiplicative rather than an additive scale. After making plots of various sets of reserve numbers, it became obvious that the distributions were often not homogeneous or unimodal even though having the general log-normal form.

If the frequency distributions of the total recoverable reserves for Western Canada is examined it is seen that the shape of the curves is more or less the same over a period of several years with some variation in the means. Both the oil and the gas data suggest bimodality but as the overall curves can be broken into many much better defined distributions for different types of oil and gas occurrence, it should be more meaningful to examine the individual cases.

Several types of oil accumulations have reserve sizes that form unimodal log-normal distributions. One of the best plots, made up of the Leduc reef oil reserves, is shown on Figure 1. This is an almost perfect unimodal, log-normal distribution made up of the probable reserves for some 52 pools. The figure shows the same data plotted in three different ways. The best method is using probability paper and is shown on the main graph in the centre of the figure, in which a log-normal distribution appears as a straight line. The geometric mean of the Leduc reef reserves can be read off at the 50 per cent mid-point of the cumulative frequency plot and is about three million barrels. The arithmetic mean (total reserves divided by number of pools) for the Leduc is about fifty-three million, and this average is obviously very misleading if it is to be considered the most likely size to be found. Any

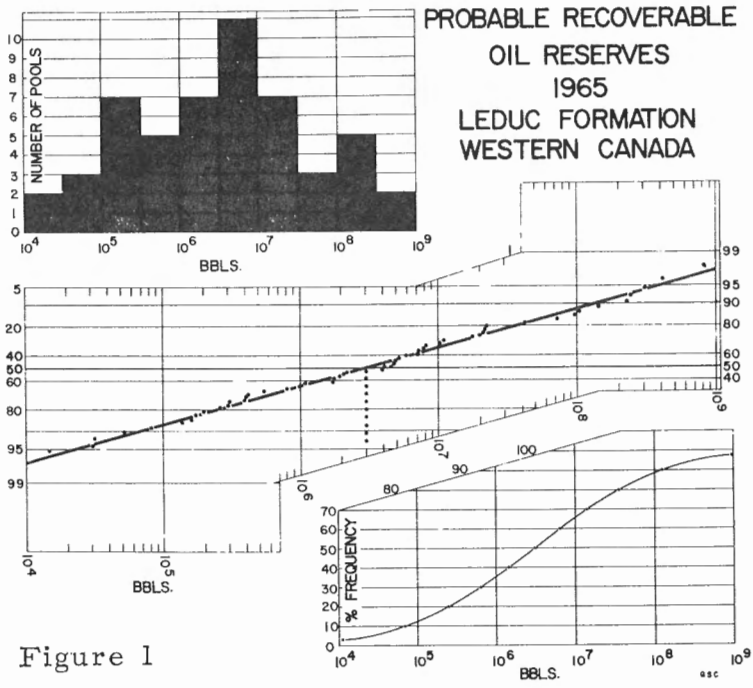

Figure 1

estimates of the size of future pools to be discovered in a play should fall into the established distribution. If they do not, they are probably unrealistic, assuming a sufficient history has been established.

Pool area is probably the variable that correlates most strongly with reserve size in Western Canada. Thus it is interesting to see the comparison of reef pool areas shown on Figure 2. The Leduc reef areas appear to be unimodally distributed but the distribution is modified at the lower end to appear truncated because of a large number of estimated values. These data are from a different source than the reserve data of Figure 1. All plots of areas tend to show values at their lower ends, rounded to well spacings that do not fit the distribution curves. Making plots of various parameters is a useful way of observing the extent of the estimations included in a given set of data and whether they are apt to be too high or too low. Estimates are made most often in the smaller pool size range and may have some bearing on the development of bimodality discussed next.

Figure 3 is a plot of the probable ultimate recoverable oil reserves from the Viking Formation and is an example of a bimodal distribution. Here, we are dealing with two overlapping log-normal distributions. The resulting curve is a mixture of 60 per cent of a population of smaller sizes, 40 per cent of a population of larger sizes. This curve can be dissected

graphically into its two component distributions. The smaller population, having a geometric mean of .3 million barrels and a larger population with a mean of 12.8 million. A calculated arithmetic mean for the larger group is 30 million barrels.

There are at least two hypothesis that would explain the heterogeneity of these distributions. First, it might be the result of some fundamental difference in the geology of the two populations, the porosity type for instance. Secondly, it might result from an inaccuracy in the estimation of one or both groups of reserves, that is, the heterogeneity could be induced. The group of larger sizes could be over-estimated which I think is the less likely situation, or the group of smaller sizes could be under-estimated. One reservoir parameter that is often approximated for smaller pools is the area and this would create a larger percentage error in a small pool than in a large one. A plot of Viking pool areas is also bimodal, suggesting that in this case area estimates must have been an important factor in creating bimodality. For the Viking it is difficult to conceive of geological reasons that would explain why the small pools should be different from the large. In other cases this may not have been so.

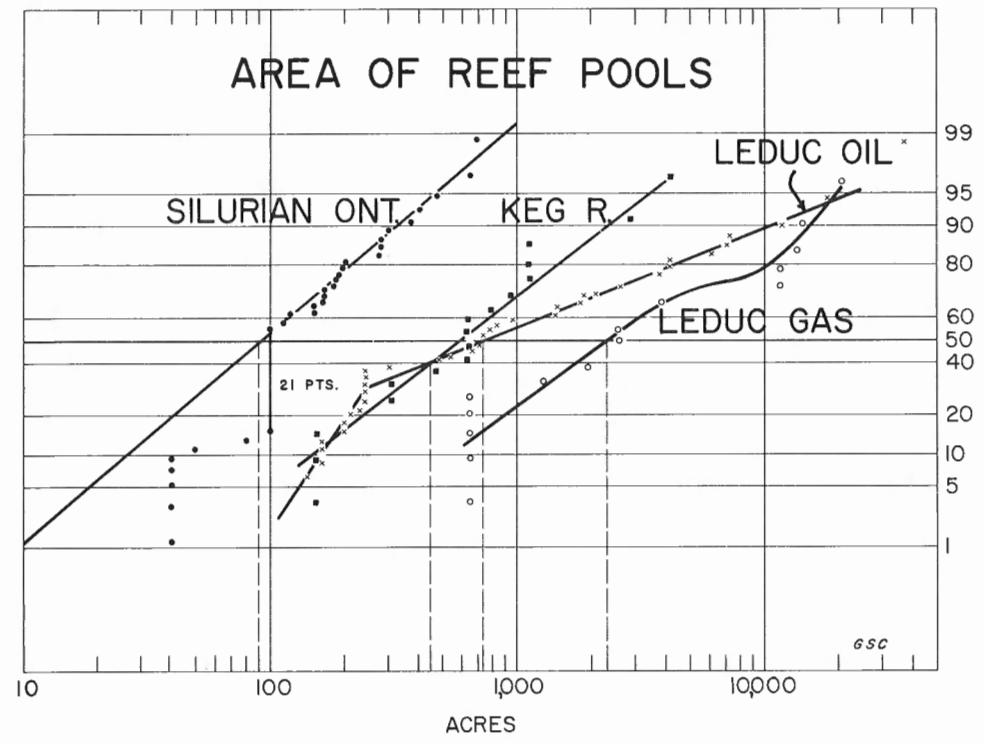

Figure 2.

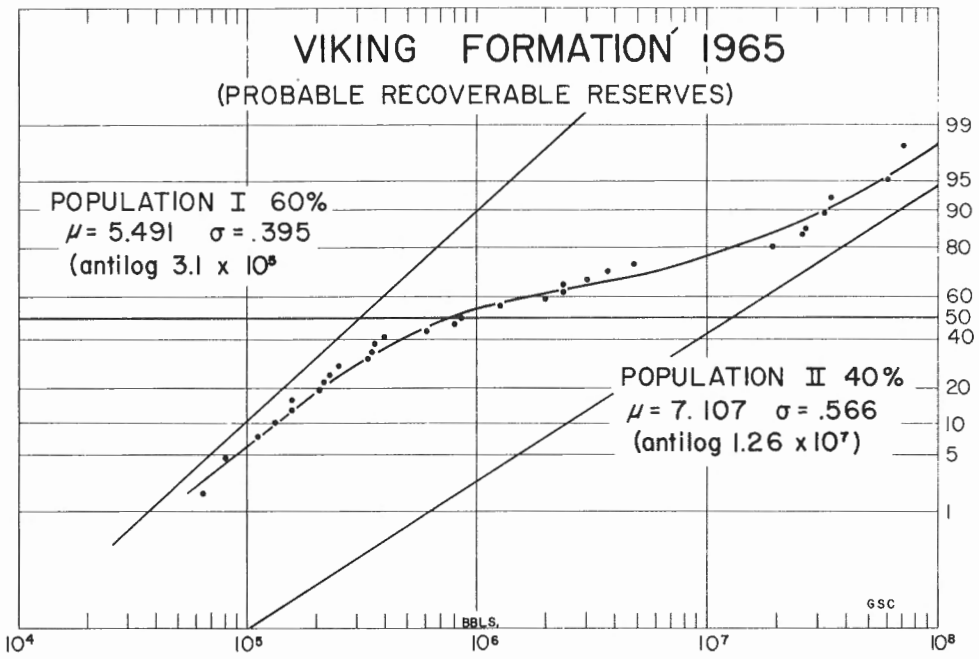

Figure 3.

In view of the foregoing consider the hypothesis that there are two populations; created in some cases, by a lack of knowledge about the smaller pools. If this is accepted, then the reserves that would be present if all the pools fell in the population II of larger sizes can be calculated. By computing the arithmetic means of population II and multiplying by the total number of pools, a postulated reserve is determined. In this case it would be 960, 000, 000 barrels, whereas the actual value, that is the total for the group of points used to make the plot, is about 300, 000, 000.

Many similar examples can be found in genetically related groups of oil and gas pools of Western Canada. Considerable variation in the parameters of these different distributions can be seen. Obviously much remains to be done on this subject, nevertheless, the topic is of sufficient current interest to warrant discussion. It would be desirable to examine all the data on the related pools to determine the degree of geological consistency within a set.

This approach should be a useful way of examining a set of data for its internal consistency. It is assumed that a geologically consistent group of pools on which the reservoir parameters have been correctly determined should form a unimodal log-normal distribution. If the distribution being examined is found to be heterogeneous, then I think one is obliged to form

some sort of opinion as to why this should be so. This may in turn draw attention to some inconsistency in the way in which these numbers have been derived or may indicate that two geologically unlike groups of pools have been grouped together. An examination of this type of plot is an excellent way of seeing whether any individual pools are too large or too small the same way we can look at a group. Even though the graphical estimates are not particularly accurate, possibly the method may have at least semi-quantitative or directional significance giving some relative idea which sets of reserve numbers are reasonably representative of the ultimate potential of a group of pools. The additional reserves postulated in the bimodal cases may not all be commercial in that many of the smaller pools in the sample on which the analysis is based may not in themselves be commercial (i.e. their pay thickness may be marginal). The degree of bimodality in the plots also may suggest the maturity of the exploration play in a particular oil and gas system. As the distribution becomes more and more completely known it should approach a unimodality.

PETROLOGY

32. WATER-RICH PARTS OF THE SYSTEM ALBITE-ORTHOCLASE-QUARTZ-WATER

K. L. Currie

The system albite-water is effectively quaternary over the range 400-650°C and 400-3,500 bars. Silica is extracted in excess of stoichiometric proportions in the lower parts of the range, and soda is extracted in the higher parts. The solubility of alumina exhibits a temperature maximum in the region of 550 degrees. The system microcline-water is similar, but the solubility of potassium is more strongly pressure dependent than is that of soda. Solutions derived from mixtures of microcline and albite show a very strong discrimination in favour of soda, with the amount of potash gradually increasing with pressure. In all three systems the solubility of silica and alumina is identical within experimental errors. The quinary system quartz-albite-microcline-water (artificial 'granite') shows a higher silica content, but is not saturated with silica, according to the data for quartz. This system likewise is enriched in soda relative to potassium at low temperature and pressure. All these systems show strong dynamic effects probably of geological importance. Under dynamic, non-equilibrium passage of solutes, silica is leached from the residues with great efficiency while the other components are virtually inert. The data show that even using leucite or nepheline as starting materials, the solutions contain sufficient silica to form feldspars.

The data have been handled theoretically by a new hypothesis on the solubility of solids in dense fluids. Starting from statistical mechanical treatment of the thermodynamics, this produces a solubility equation depending only on pressure and temperature. This equation satisfactorily handles the present data.

33. MINERALOGICAL STUDIES OF THE MANICOUAGAN STRUCTURE, QUEBEC

K. L. Currie

The central parts of the Manicouagan octagonal structure contain areas of anomalous minerals, displaying aberrant optical and X-ray properties[1]. Plagioclase, potash feldspar, biotite, amphibole, pyroxene and garnet have been studied in some detail. The effects in plagioclase are decreased birefringence (locally to the point of isotropy), anomalous dispersion, and greatly decreased optic angle. X-ray analyses of anomalous feldspars are those of extreme high-temperature plagioclase, with some marked broadening of diffraction peaks. Double variation optical study of plagioclases shows that birefringence is decreased by approach of the 'b' and 'c' indices to each other while the 'a' index is relatively unaffected. This is interpreted to be due to fine recrystallization about the 'a' axis with the 'b' and 'c' axes relatively randomly distributed. This effect is accompanied by somewhat erratic decrease of optic angle. Uniaxial (!) plagioclases then show a decrease of index of the 'b-c' ray finally reaching isotropy with an index near or just below that of the 'a' ray. Diopside shows effects very similar to those in plagioclase, and the uniaxial stage is commonly found. As yet no isotropic pyroxene has been found. Oxidation of the small amount of iron in these pyroxenes produces a yellowish colour and a noticeable expansion of unit cell volume. Biotite and amphibole display prominent 'kinking' of the cleavage and patchy areas of reduced birefringence. Both minerals are almost entirely oxidized to hematite. Both were particularly subject to vesicular vitrification, and are represented in the most altered zones by vesicular brown glass.

---

[1] Currie, K. L., and Murtagh, J. G.: Preliminary map of the Manicouagan structure; Geol. Surv. Can., Paper 67-70 (in press).

34. STUDIES IN THE SYSTEM Na-Al-Si-F-H_2O

K. L. Currie

Phase equilibrium studies in systems with the composition albite plus fluorine have been begun using mixtures of silica gel, alumina, sodium peroxide and sodium fluoride. Dry systems react very slowly even at 700 degrees, but the equivalent hydrous system readily reacts in one week at 400 degrees. Thus far only albite has been found at total pressures above 1 kilobar, but at lower pressures another unidentified mineral, possibly a fluor-muscovite is present.

35. STUDY OF DYKES IN THE FRANCON QUARRY, OTTAWA

K. L. Currie

A system of narrow 2-inch to 1-foot dykes cross the Francon Quarry which is situated in Ordovician limestones. The dykes consist of many rounded fragments of exotic rocks in a fine carbonate matrix. Studies have shown that some of the fragments are of altered alkaline rocks, while others seem to be normal granitoid gneisses. Fragments of the surrounding limestone are not common except at the margins. Many of the dykes show a well-developed fine vesicular flow structure. Two drilled specimens display a very stable remnant magnetization giving a Cretaceous pole direction. The dykes display a marked radioactivity concentrated in the carbonate matrix. Phenocrysts (xenocrysts?) of biotite display unusual optical characters varying from normal at the centre to anomite type optics at the edges. The data support the hypothesis that the dykes are carbonatite, possibly related to the Monteregian petrographic province. The hypothesis that the dykes are of clastic origin accords poorly with the facts.

PRECAMBRIAN GEOLOGY

36. GOLD-ARSENOPYRITE-LOELLINGITE-PYRRHOTITE DEPOSITS IN AMPHIBOLITE, ITCHEN LAKE-CONTWOYTO LAKE AREA, DISTRICT OF MACKENZIE

H. Bostock

Introduction

In the course of 4-mile reconnaissance mapping in the Itchen Lake area[1], samples containing arsenopyrite and loellingite were collected from the following localities: (1) claims held by Giant Yellowknife Mines near Point Lake, 6 miles south of the mouth of Itchen River; (2) the Fuz claims held by International Nickel Company 4 miles north of Itchen Lake; and (3) International Nickel Company main showing near the northeast end of Contwoyto Lake. These deposits are of particular interest because they contain gold.

This paper describes the textural relations of arsenopyrite and loellingite, and reports on the distribution of visible gold with respect to the major minerals present in the samples collected. An interpretation of the data together with the results of investigations of mineral proportions, trace element distribution, and sulphur isotope ratios in sulphides will be the subject of a later publication.

General Geology

Arsenopyrite-loellingite mineralization at these localities is confined to local occurrences within layers and lenses of iron sulphide bearing amphibolite that are mostly less than 60 feet thick and are interbedded with pelitic to psammitic sediments. This assemblage forms a mappable unit that can be traced from south of Point Lake northward and eastward at least as far as the southeast shore of Contwoyto Lake. To the south it appears to be overlain by similar rocks which lack bands of amphibolite. To the north it passes into heterogeneous granitic rocks by migmatization and intrusion, accompanied by deformation. Near the north arm of Point Lake, sulphide-rich lenses become rare and magnetite is prominent in association with amphibole. The assemblage of lithologies which form this unit are thought to constitute the metamorphic equivalents of an oxide-silicate-sulphide facies of iron-formation. The unit appears to be stratigraphically equivalent to part of the

volcanic succession at the base of the Yellowknife Group at Point Lake. The regional geology and further details of these lithologies are given by Bostock[1, 2] and Tremblay[3, 4].

Mineral Relations

The sulphide-bearing amphibolite, where least deformed, is composed predominantly of silicates, but bands or lenses variably enriched in pyrrhotite and/or pyrite of different grain sizes are interleaved. Chalcopyrite makes up 1 or 2 per cent by volume of the total sulphides in all samples.

These minerals occur chiefly as blotches, commonly up to 1/2 inch in length, that are aggregates of euhedral (somewhat stubby diamond-shaped) to anhedral crystals. Blotches occur in bands parallel to bedding, and in patches more or less independent of bedding. Nearly massive arsenopyrite-loellingite and, less commonly, vein-like bodies cutting across beds were also observed. Blotches are typically more or less elongate parallel to foliation or bedding in the host rock; however some were observed in gash-like lenses, and other exceptions are not uncommon.

In detail, arsenopyrite-loellingite blotches consist of clusters of more or less euhedral arsenopyrite crystals that surround corroded anhedral remnants of loellingite distributed in symmetrical or asymmetrical arrays (see Figs. 1, 2). Isolated blotches of arsenopyrite-loellingite (without associated pyrrhotite) in rare instances have loellingite in direct contact with silicates. Loellingite rarely occurs in contact with pyrrhotite and then only where small bodies of pyrrhotite, apparently included in loellingite, are incompletely rimmed by arsenopyrite. Loellingite in contact with pyrite was not observed. Interstices between arsenopyrite-loellingite crystals within blotches are occupied primarily by pyrrhotite or pyrite, and by chalcopyrite. The ratio of chalcopyrite to pyrrhotite or pyrite appears to be greater within blotches than in the surrounding rock.

Pyrrhotite both within and remote from arsenopyrite-loellingite blotches typically shows some evidence of late incipient alteration to pyrite. In some samples botryoidal pyrite has formed along fractures and grain boundaries so that pyrrhotite is restricted to the remnant centres of original crystals; in others the alteration is confined to tiny botryoidal growths along cracks and grain boundaries which are outlined by pitted haloes in pyrrhotite (see Fig. 3); in still other samples no late pyrite is evident but short tiny cracks of subequal length penetrate surrounding pyrrhotite at right angles from grain boundaries and fractures.

Microscopic gold grains were observed in all but one of the samples of arsenopyrite-loellingite studied. Counts indicate that about 70 per cent of all observed gold grains are present at the boundaries between arsenopyrite

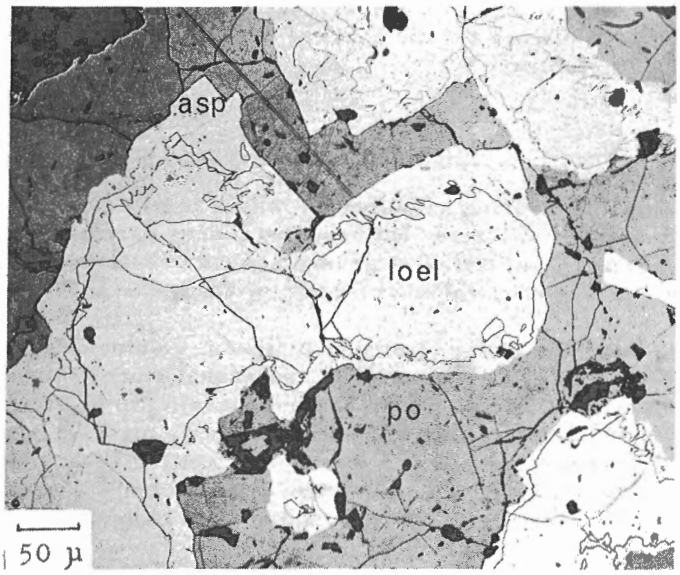

Figure 1. Arsenopyrite (asp)-Loellingite (loel) intergrowth in pyrrhotite (po) from Fuz showing. (GSC 200211-I).

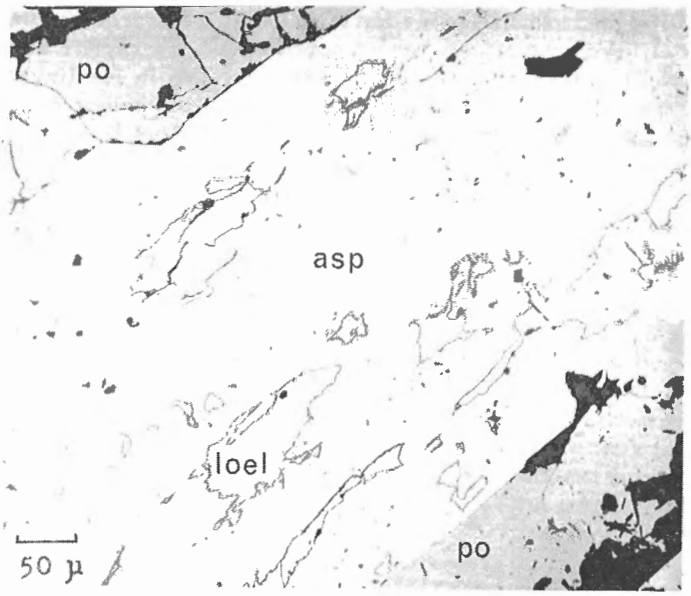

Figure 2. Arsenopyrite (asp) – Loellingite (loel) intergrowth in pyrrhotite (po) from main showing. (GSC 200822-D).

and loellingite (see Fig. 4). Since the grains at this boundary are typically larger than those elsewhere, much more than 70 per cent of the visible gold is present at the arsenopyrite-loellingite boundary. Gold grains within loellingite (about 10 per cent of visible gold grains) generally resemble those at the grain boundaries but are usually smaller, and in some cases lie in fractures that terminate at the arsenopyrite-loellingite boundary. Gold grains in arsenopyrite (20 per cent of visible gold grains) are typically much smaller than those at the arsenopyrite-loellingite boundary (commonly 0.0002 mm^2 or less in section). In comparison with gold elsewhere their boundaries commonly appear ragged. Very little gold is present at the arsenopyrite-pyrrhotite boundary and those grains observed were associated with small bodies of pyrrhotite apparently included in arsenopyrite. No gold was observed at other sulphide boundaries. Gold at intersilicate boundaries is prominent in one sample from Fuz showing.

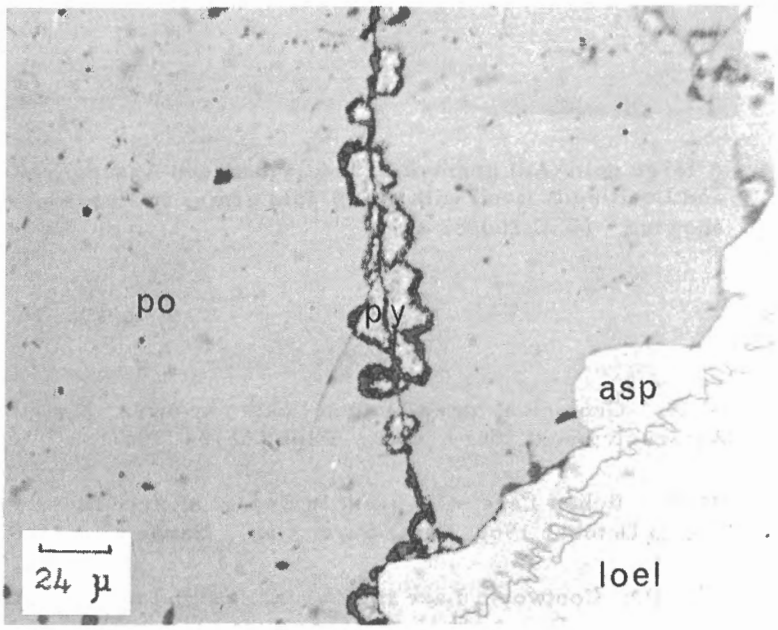

Figure 3. Pyrrhotite (po) altered to pyrite (py) along fractures and grain boundaries Inco main showing. (GSC 200822-E).

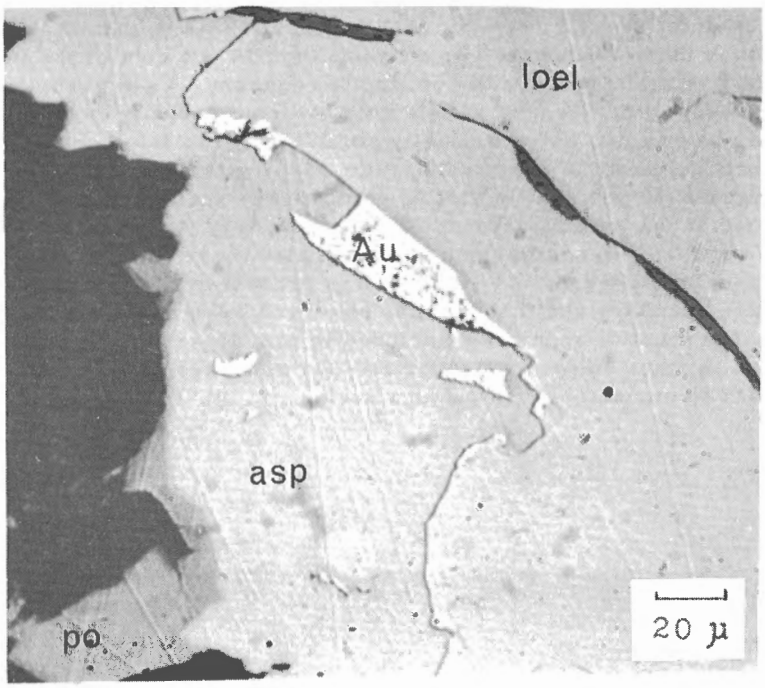

Figure 4. A large gold (Au) grain at boundary between Arsenopyrite (asp) and Loellingite (loel) with small gold grains in Arsenopyrite, Fuz showing. (GSC 200822-C).

[1] Bostock, H.H.: Geological notes, Itchen Lake map-area, District of Mackenzie; Geol. Surv. Can., Paper 66-24 (1967).

[2] Bostock, H.H.: Itchen Lake map-area; in Report of Activities, Part A: May to October 1966; Geol. Surv. Can., Paper 67-1 (1967).

[3] Tremblay, L.P.: Contwoyto Lake map-area, District of Mackenzie; Geol. Surv. Can., Paper 65-21 (1966).

[4] Tremblay, L.P.: Contwoyto Lake area (north half), District of Mackenzie; Geol. Surv. Can., Paper 66-28 (1967).

37. FUNNEL GRABENS IN THE THELON FORMATION

J. A. Donaldson

Conical collapse structures that occur in flat-lying Cambrian sandstones of Sweden have recently been described by Lindström[1], who termed such structures 'funnel grabens'. Similar structures occur in sandstones of the flat-lying Proterozoic Thelon Formation of the Dubawnt Group, Northwest Territories.

Figure 1 illustrates one of three funnel grabens observed in the Thelon Formation, the regional geology of which has been outlined elsewhere[2]. The Thelon funnel grabens are circular in plan, have a maximum diameter of 20 feet, and exhibit inward bedding inclinations of up to 40 degrees. Bedding is distinct, shows no evidence of attenuation or disruption, and is transected by joints that post-date the funnel grabens. The structures appear to have formed when the sand was consolidated sufficiently to maintain bedding coherence, but before it was lithified sufficiently to fracture.

Lindström[1] attributed formation of the funnel grabens in Sweden to tectonic movements that occurred before the sandstones were fully consolidated. He suggested that opening of fractures in the basement allowed downward movement of mobilized sand, thus leading to formation of the funnel grabens. Those in the Thelon Formation are in proximity to the northeastward extension of the MacDonald Fault, and therefore a similar origin seems likely.

---

[1] Lindström, Maurits: "Funnel grabens" and Early Paleozoic tectonism in south Sweden; Bull. Geol. Soc. Am., vol. 78, pp. 1137-1154 (1967).

[2] Donaldson, J. A.: Two Proterozoic clastic sequences: a sedimentological comparison; Geol. Assoc. Can., vol. 18, pp. 33-54 (1967).

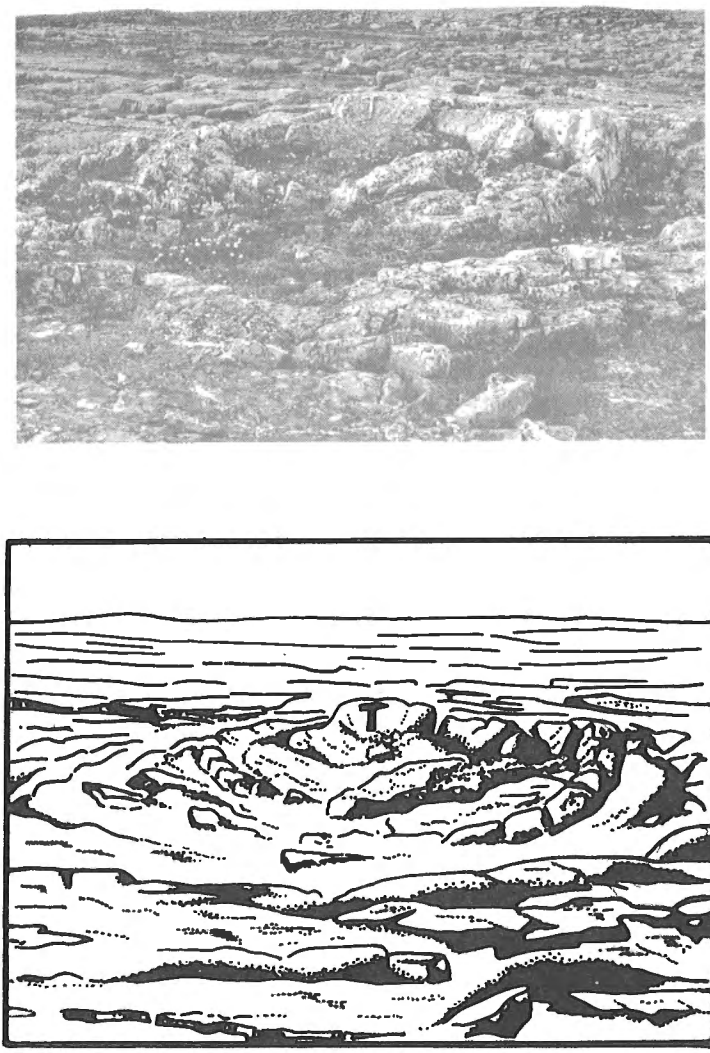

Figure 1. Funnel graben in Thelon Formation, 2 miles southeast of Grassy Island on Thelon River (Station DF-A760-65; coordinates 63°45'00"N, 104°17'05"W). Hammer rests on inward-dipping bed.

QUATERNARY RESEARCH AND GEOMORPHOLOGY

38. GEOMORPHOLOGICAL MAP OF THE GATINEAU PARK

Jane T. Buckley

A preliminary geomorphological map of the Gatineau Park was completed in manuscript form at the request of the National Capital Commission, Division of Long Range Planning. A brief written account accompanied the map.

Field work, carried out during June, July and August 1967, was followed by a thorough airphoto interpretation using photography flown in November 1966 from 9,000 feet altitude. Preliminary mapping was completed at a scale of 1:25,000 for reduction to 1:50,000.

The map shows landforms and surface deposits, including glacial, glaciofluvial and marine-modified glaciofluvial features and deposits; freshwater deposits, quarries, dams, etc. Little is shown of slope angles or lengths, besides the outlining of the active stream-valley slopes and the edges of the major terraces. Groundwater information is not included.

A shell sample collected from south of Meach Lake has been dated at 11,600 ± 150 years B.P. (GSC-842) which provides the oldest known date to be associated with the near maximum elevation of the former Champlain Sea in the Ottawa area. Previously the maximum age in this area was established at 11,320 ± 200 years B.P. (L-639 B), from shells found by Terasmae at Kingsmere Pits. The upper limit of the Champlain Sea has been defined in an embayment northwest of Wakefield, bordering the Gatineau Park. Shells found just south of Lake Mahon are believed to relate to the time when the sea stood at this upper limit.

39. GRADIENTS OF PAST AND PRESENT OUTLET GLACIERS

Jane T. Buckley

Measurements of the overall gradients of outlet glaciers have revealed a direct relationship between overall length and gradient of glaciers flowing from inland icecaps to fiords. Maps at a scale of 1:250,000 were used in few areas of study: (1) the coastal area of Alaska, including the 'Panhandle'; (2) the entire coastal strip of Greenland; (3) the Transantarctic Mountains between 76°S and 84°S in Antarctica; and (4) the eastern part of the Canadian Arctic Archipelago. All these areas have glaciers flowing between icecaps and fiords, and also have numerous glaciers flowing from mountain headwalls to fiords. Diagrams showing the cumulative percentage of the total height gained at 5-kilometre intervals along the profile, were grouped according to similarity of profile. The best-fit curve for each group was then calculated together with its standard error limits.

The results obtained from this analysis have an application in the problem of reconstructing former ice-surfaces such as that which lay over northeastern Canada at the maximum extent of the Wisconsin glaciation. Former ice-surfaces have been reconstructed for Sam Ford Fiord in Baffin Island, where existing old moraines on the outer coast have been used in fitting constant gradient and average profile surfaces to the known length of the fiord. The results suggest strongly that many of the highest mountain peaks on the outer coastal fringe of Baffin Island remained ice-free during the Wisconsin glacial maximum.

40. PALYNOLOGICAL STUDIES AND STRATIGRAPHIC DRILLING, ONTARIO

J. Terasmae

A 60-foot bed of pollen bearing sediments at a depth of 120-180 feet in the buried St. David's gorge of the ancient Niagara River has yielded palynological assemblages indicative of boreal forest vegetation and a corresponding cool climate during the deposition of this stratigraphic unit. A radiocarbon date of 22,800 $\pm$ 450 years B.P. (GSC-816) was obtained for woody detritus from this bed. Glacial deposits occur both above and below this unit. The studies made indicate that the St. David's gorge was cut prior to the last glaciation (Wisconsin), probably during the Sangamon interglacial interval – or earlier.

The stratigraphic drilling at Hamilton-Dundas, Ontario, was undertaken during the winter of 1967-68 to investigate the stratigraphy of surficial deposits in a buried valley, which according to geophysical studies made by G. D. Hobson and previous drilling records, extends from Dundas to the Burlington Skyway where it enters the Lake Ontario basin. Preliminary results indicate that a stratigraphic sequence of surficial deposits similar to that compiled for the Hamilton area by P. F. Karrow is present in the buried valley. Several gravel units at depth contained groundwater under pressure. It is possible that these aquifers could be utilized as a possible source of water supply.

Sediment cores were collected through the ice in several lakes in the Kingston-Belleville area, Ontario, for a study intended to establish the radiocarbon age of surface sediment. A necessary reference datum for this study is provided by the sudden rise in the Ambrosia (ragweed) pollen abundance, near the top of the sediment core (mud/water interface) and related to the settlement of the area. An absolute age for this datum can be obtained from historical records and radiocarbon determinations can be calibrated against this known age. Similar studies made in recent years (e. g. in Ohio by G. J. Ogden) have clearly established the need and usefulness of this approach to dating of lake sediments. Ogden has shown that surface sediment in lakes can often have a radiocarbon age of several hundred years and hence, dates obtained for samples of lake bottom deposits can lead to misinterpretations in the geochronological context.

STRATIGRAPHY AND PALEONTOLOGY

41. FORAMINIFERA USEFUL FOR DETERMINING THE JURASSIC-CRETACEOUS BOUNDARY IN ARCTIC AMERICA

T. P. Chamney

The coarse clastic lithology and predominantly non-marine nature of the sediments deposited at the close of the Jurassic and into the Cretaceous over the Canadian Western Interior has in most areas precluded the application of foraminiferal control for age dating and correlation. A continuous depositional sequence through this interval with argillaceous lithologies and marine conditions has been studied close to the boreal marine source in Arctic America. The area includes a belt of exposed strata trending northeastwards from the mainland of Canada in the vicinity of the Mackenzie River Delta to the Sverdrup Basin of the Arctic Islands in the vicinity of western Ellesmere Island.

The litho-stratigraphic problem of this boundary interval results from the contact being contained within the rather homogeneous shale sequences of the Deer Bay and Mould Bay Formations. On the mainland in the Richardson Mountain area the equivalent biostratigraphic interval is within the Husky Formation[1].

Lower Cretaceous

Lituotuba spp. – Early Neocomian (Valanginian or Berriasian)

Acme of occurrence of this genus with forms referred to Lituotuba irregularis Tappan and a new species.

Upper Jurassic

Arenoturrispirillina n. sp. 2 – Late Portlandian

Arenoturrispirillina n. sp. 1 – Early Portlandian

Middle Jurassic

Ammodiscus n. sp. 1 – Callovian or Late Bathonian (Wilkie Point or Upper Savik Formation)

The species of Foraminifera selected for this report are but a few of the more diagnostic forms. The genus Arenoturrispirillina is most distinctive and has never been previously reported from the Mesozoic of America. The new species of Ammodiscus is 4 mm in diameter which places it as a giant, some 2.5 mm larger than any previously reported Mesozoic species. Although species of Lituotuba are fairly common throughout the Mesozoic,

never has such an acme of occurrence been recovered from the sediments of the Canadian Western Interior or Arctic America. By reason of the most distinctive features, these new species are considered to be useful in determining a position in the vertical stratigraphic sequence without the necessity of detailed speciation of the abundantly associated common microfaunal elements that include Haplophragmoides, Trochammina and Gaudryina.

---

[1] Jeletzky, J. A.: Jurassic and (?) Triassic rocks of the eastern slope of the Richardson Mountains, northwestern District of Mackenzie, 106M and 107B (parts of); Geol. Surv. Can., Paper 65-50, Fig. 30 (1967).

---

42. AUTOEMULSIFICATION FOR DISINTEGRATION OF ARGILLACEOUS ROCKS

T. P. Chamney

Highly calcareous shales and other mineralized argillaceous rocks, are most difficult to disintegrate for the extraction of microfossils. The argillaceous fraction of these rocks will not go into solution with the application of the commonly used ionic dispersal reagents (super detergents). Stronger reagents of a caustic or acid nature cannot be employed because of the calcareous composition of the microfossil shells of some classes of these organisms.

The principle of autoemulsification has recently been used for disintegrating non-swelling lattice clays and calcareous shales. Autoemulsification takes place between a hydrocarbon solvent and water when the two hot reagents are applied in sequence to an argillaceous rock. An emulsion is produced by the interaction of surface tensions and capillary forces within the minute rock passageways. The solvent action of the hydrocarbon plus the internal forces generated by the autoemulsification within the rock particles will, with repeated applications, produce an acceptable disintegration. This is a very time-consuming operation requiring handling of the sample for each application. After hydrocarbon saturation of the sample the excess solvent requires decanting and filtering. After addition of the water, the sample requires treatment with ionic dispersal reagents to eliminate the hydrocarbon for filtering and screening. The sample must be thoroughly dried after each autoemulsification before proceeding with repeated applications.

The new autoemulsification procedure developed by the Institute of Sedimentary and Petroleum Geology is a continuous process in a closed system of repeated hydrocarbon and water wetting, obviating the necessity of physically handling the rock sample after each application. The equipment, illustrated in Figure 1, consists of a Kontes quadruple head clamped to a beaker which makes up the reaction flask. This is a single retort of the pilot model but in operation as many retorts as required can be arranged with a vapour collecting system connected to the condenser. The fumes could be exhausted through a fume cupboard but in quantity processing, recovery of the hydrocarbon solvent is economical and valuable fume cupboard space is not permanently occupied.

In operation the crushed rock sample is boiled in hydrocarbon solvent in the reaction flask for approximately ten minutes. A predetermined quantity of water is then permitted to flow into the reaction flask, sufficient to completely cover the sample as it displaces the hydrocarbon. The interaction between the two liquid interfaces proceeds until the water has been boiled off. Visual observation of the sample is difficult but the status of the liquid phases is indicated by the temperature in the reaction flask. The fourth neck of the Kontes quadruple head holds a thermometer and a rise in temperature above the boiling point of water indicates the hydrocarbon solvent phase is in contact with the sample. The procedure is repeated until the rock matrix is sufficiently weakened and the sample crumbles into a mushy mass. If the lithology of a rock is at all amenable to disintegration, approximately six applications of the water phase should produce the desired results.

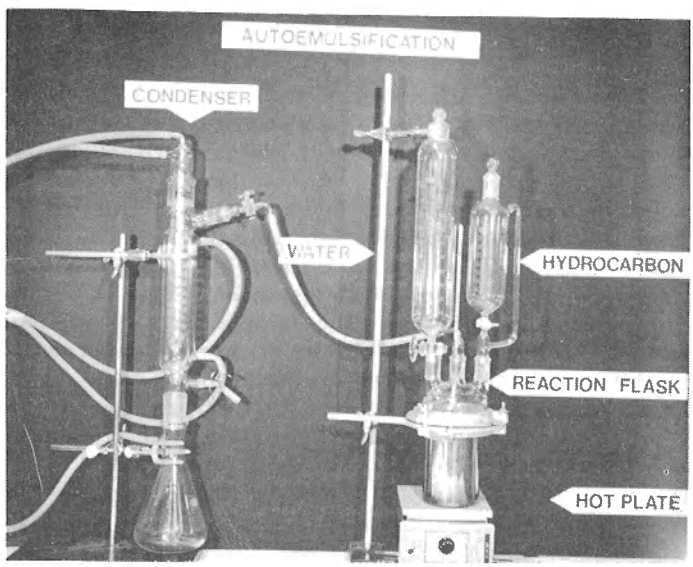

Figure 1.

Autoemulsification equipment.

43. LOWER CARBONIFEROUS (MISSISSIPPIAN) FORAMINIFERA OF SOUTHWESTERN ALBERTA

A. A. Petryk

Continued progress has been made in this study which began in June 1966[1]. In the summer of 1966 about 6,000 samples from 32 stratigraphic sections were examined and about 700 thin sections prepared. Some 1,800 photomicrographs were taken and printed at the University of Saskatchewan, Saskatoon, during the spring 1967. Since then a taxonomic analysis has been made.

To date, taxonomic evaluations and descriptions are tentatively completed. In the families Fischerinidae (Cornuspiridae), Tournayellidae, Paleotextularidae, Endothyridae, Bradyinidae, Eostaffellidae nom. nud. Mamet, Tetrataxidae, Archaediscidae, Earlandiidae and Incertae Sedis (Calcispheres etc.), about 40 genera and 100 species were identified. They range from the Middle Tournaisian (Tn2) to the Upper Visean (V3cj), Osage to Lower Chester of the Mississippi Valley sections.

Most of the genera are cosmopolitan[2]. Specific differences on an intercontinental, regional and local basis are remarkable. Correlation, however, is readily made by combining common characters into larger species groups. In the next phase of this study, to be done at the University of Saskatchewan, foraminiferal assemblages will be used to derive the biostratigraphic zonal scheme.

---

[1] Petryk, A. A.: Mississippian foraminifera of southwestern Alberta; Geol. Surv. Can., Paper 67-1, Pt. A, p. 105 (1967).

[2] Mamet, B., and Skipp, B.: Lower Carboniferous calcareous foraminifera: Preliminary zonation and stratigraphic implications for the Mississippian of North America (in press).

GENERAL

44. PHOTOGRAPHY OF GRAPTOLITES

F. J. Cooke

Geological photographers are frequently required to produce excellent pictures from extremely low contrast media, and it is to their credit that they have had considerable success, having evolved such methods as ammonium chloride coating, various oil immersion methods, infrared photography, and weird film and filter combinations and indeed everything was under control until the 'Graptolite' was introduced to the camera technician. All the time-honoured methods failed to produce satisfactory pictures from most graptolite specimens. What was needed was a foolproof system that would produce reproduction quality prints of all graptolite specimens regardless of any physical condition of rock surface or specimen preservation. Accordingly, a new method has been worked out at the Geological Survey of Canada, which will produce excellent prints no matter how low the contrast of the specimen.

The Method

The whole operation is photographically unorthodox. Because specimen contrast is near zero, a film with a high inherent contrast was a necessity, and thus for our initial test we chose contrast process panchromatic film, the theory being that this film would provide the contrast lift that was absent from the specimen. If correctly processed, this film would produce too much contrast, and produce a picture that would be too black to reproduce. To prevent this, we processed our film in a soft working developer, namely D 76, a borax solution. This proved to be a good choice, our negative was tamed to the point of perfection, development time was five minutes at 70 degrees, approximately half the normal processing time. The fine grain structure of the film resolved the minute detail of the specimen beyond imagination; the negative could only be described as exceptional, contrast separation was unique.

Lighting and Equipment

The method is only as good as the camera and lens can make it and certainly the customary or usual camera and photo-flood lamps will not produce the effect described here (see Figs. 1, 2, and 3); in fact it is impossible

to photograph many specimens with ordinary equipment. Since many specimens must be enlarged through the camera, macro lenses and flexible lighting is mandatory. We used a vertical macro camera and very good macro lenses, and as these lenses are ground to work at close proximity to the specimen, good relief and definition is assured. It must be admitted however that the light source is important. We have found that point source illumination is to be avoided, and we use two seven watt daylight fluorescent lamps for two reasons, first they seem to permit a deeper exposure penetration, and where a specimen is situated in a seedy or sandy rock, the softness of the light prevents much of the flare and surface reflection common to point source illumination. A further asset is that these small lamps permit placing the lights at angles that would be impossible with conventional equipment. The great advantage to the photographer using a vertical macro camera is that he can watch the ground-glass while moving the lights, thus arriving at the best angle quickly while sitting comfortably in front of the camera.

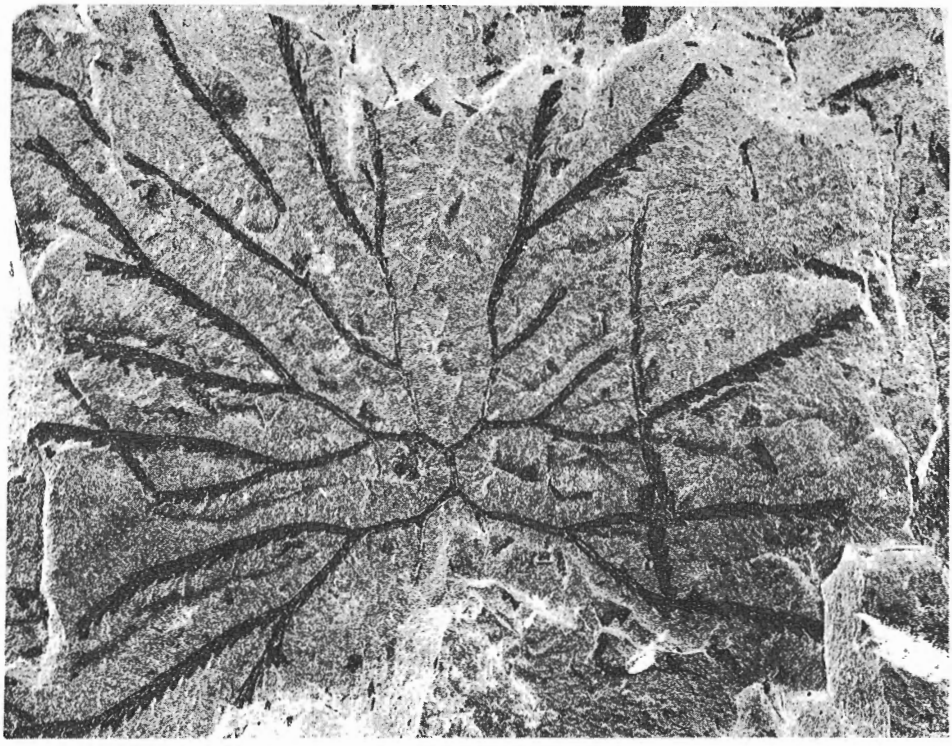

Figure 1. Example of black graptolite in black shale.

Figure 2. Example of grey graptolite in medium grey shale.

Exposure

When photographing a black specimen in black shale, the exposure must be sufficient to register good density in the black – be sure to give plenty of exposure. If you expose by light metre reading from the reflecting surface, then compute exposure increase for magnification factor. You will find it necessary to use a further factor of about three – this will account for the reciprocity factor. Filters are not required.

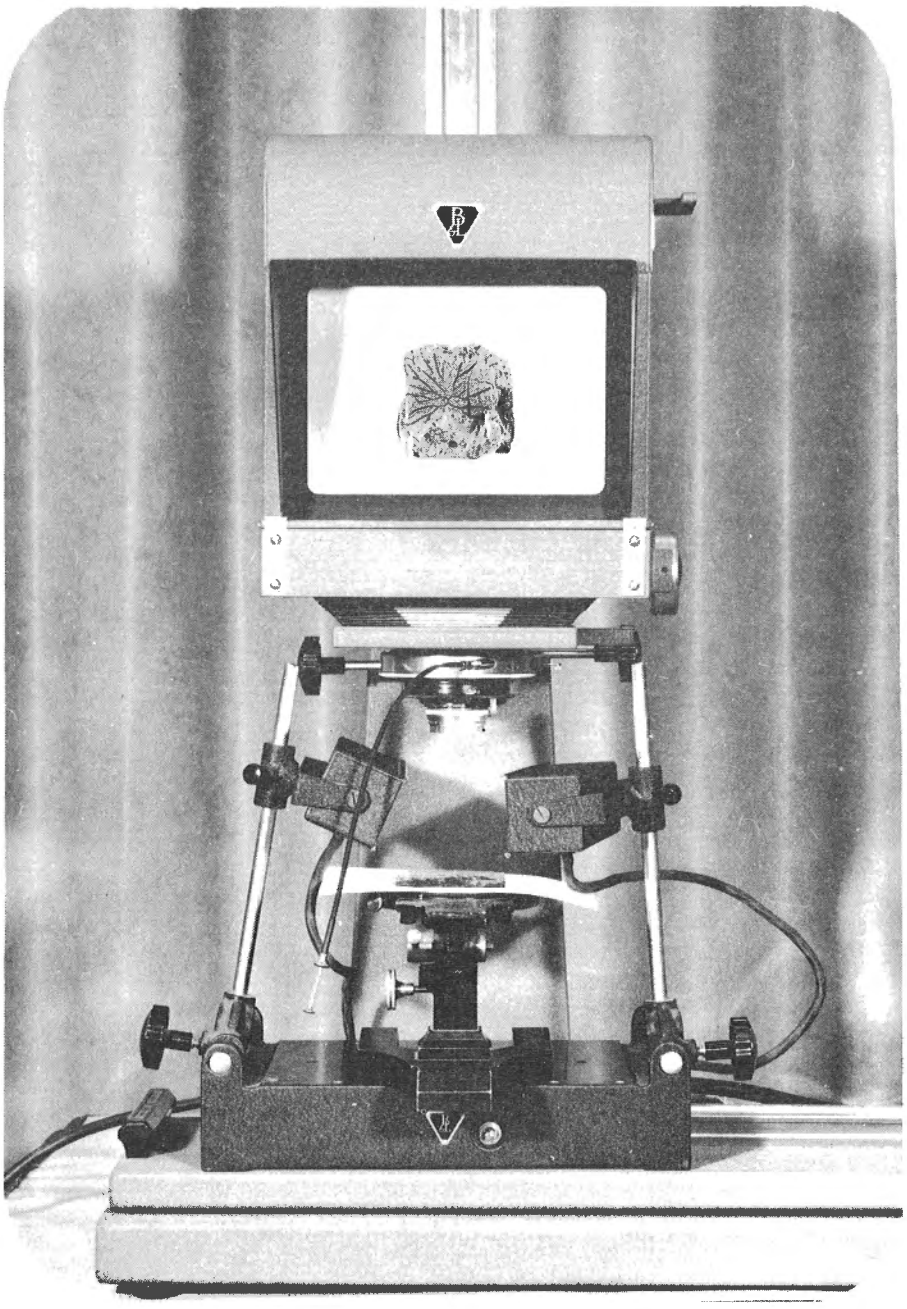

Figure 3. Vertical macro camera in working position.